QUANTITATIVE ANALYSIS OF SHAPE CHANGES IN THE CEREBRAL CORTEX ACROSS THE ADULT HUMAN LIFESPAN

by

Sourav Ranjan Kole

A dissertation submitted to the faculty of
The University of Utah
in partial fulfillment of the requirements for the degree of

Doctor of Philosophy

Department of Bioengineering

The University of Utah

December 2015

The University of Utah Graduate School

STATEMENT OF DISSERTATION APPROVAL

The dissertation of **Sourav Ranjan Kole**

has been approved by the following supervisory committee members:

Richard Daniel King	, Chair	**08/10/15** Date Approved
Alan Dale Dorval II	, Member	**08/25/15** Date Approved
Preston Thomas Fletcher	, Member	**08/10/15** Date Approved
Norman Foster	, Member	**08/10/15** Date Approved
Sarang Joshi	, Member	Date Approved

and by **Patrick Tresco**, Chair/Dean of the Department/College/School of **Bioengineering**

and by David B. Kieda, Dean of The Graduate School.

ABSTRACT

Neurodegenerative diseases are an increasing health care problem in the United States. Quantitative neuroimaging provides a noninvasive method to illuminate individual variations in brain structure to better understand and diagnose these disorders. The overall objective of this research is to develop novel clinical tools that summarize and quantify changes in brain shape to not only help better understand age-appropriate changes but also, in the future, to dissociate structural changes associated with aging from those caused by dementing neurodegenerative disorders. Because the tools we will develop can be applied for individual assessment, achieving our goals could have a significant clinical impact. An accurate, practical objective summary measure of the brain pathology would augment current subjective visual interpretation of structural magnetic resonance images.

Fractal dimension is a novel approach to image analysis that provides a quantitative measure of shape complexity describing the multiscale folding of the human cerebral cortex. Cerebral cortical folding reflects the complex underlying architectural features that evolve during brain development and degeneration including neuronal density, synaptic proliferation and loss, and gliosis. Building upon existing technology, we have developed innovative tools

to compute global and local (voxel-wise and regional) cerebral cortical fractal dimensions and voxel-wise cortico-fractal surfaces from high-contrast MR images. Our previous research has shown that fractal dimension correlates with cognitive function and changes during the course of normal aging. We will now apply unbiased diffeomorphic atlasing methodology to dramatically improve the alignment of complex cortical surfaces. Our novel methods will create more accurate, detailed geometrically averaged images to take into account the intragroup differences and make statistical inferences about spatiotemporal changes in shape of the cerebral cortex across the adult human lifespan.

Family

TABLE OF CONTENTS

LIST OF TABLES

LIST OF FIGURES

ACKNOWLEDGMENTS

First and foremost, I would like to offer my gratitude to my advisor, Dr. Richard King. While being under the tutelage of Dr. King over the past five years, I have come to know him not only as an intellectual powerhouse at our lab and at the clinic, but more importantly, as a genuinely kind and compassionate individual. His steady encouragement and support throughout this time has allowed me to flourish as an independent scientific researcher and has led me to have a well-rounded experience during my graduate studies. For all of this, and more, Dr. King, I thank you.

I offer my gratitude to the members of my Supervisory Committee, Drs. Alan Dorval, P. Thomas Fletcher, Norman Foster, and Sarang Joshi for their guidance, support, and thoughtful, incisive questions during group and one-on-one meetings, all of which has immeasurably increased the quality of my research and experience.

The research presented in this dissertation could not have been accomplished without the essential contributions of several of my fellow students and co-workers at our lab, the Center for Alzheimer's Care Imaging and Research (CACIR), and the Scientific Computing and Imaging Institute (SCI) at the University of Utah. I thank Carena Kole, my wife and with

whom I jubilantly share my life, for her meticulous and diligent work as a researcher in our lab. The innumerable hours that she has spent on almost every aspect of the projects that she has worked on have been instrumental to the success of each one of those projects. I thank Dr. Angela Wang for being a cogent soundboard throughout my graduate work, and for her generous help on many projects. I thank Dr. Nikhil Singh for the numerous constructive discussions that I have had with him and particularly for helping me to learn how to use and the tailor the use of Altaswerks for my applications. I thank Sam Preston and the SCI Support team for their help in solving several computational challenges that I had encountered. Special thanks to Dr. Denise Park, PI of the Center for Vital Longevity at the University of Texas at Dallas, for providing access to the Dallas Lifespan Brain Study database, upon which much of this work has been built.

Finally, I thank my family, Phullara Kole, Dr. Chittaranjan Kole, Devleena Kole, and Carena Kole, to whom this dissertation is dedicated. Their deeply held conviction in my abilities continues to empower my strides in life. Thank you for your love, support, and sacrifice.

This work has been supported in part by CACIR, and grants from the Robert Wood Johnson Foundation, National Institute of Aging (5-R37-AG006265-27, 5-P30-AG012300-15, and K23-AG03835), and the Alzheimer's Association.

CHAPTER 1

INTRODUCTION

This dissertation aims to outline the independent research conducted to develop novel clinical tools that summarize and quantify age-related changes in the shape of the human cerebral cortex across the adult human lifespan.

1.1 Motivation and Significance

Neurodegenerative diseases are an increasing health care problem in the United States. Alzheimer's disease (AD) is the most common neurodegenerative disease and the 6th leading cause of death in the United States of America with 84,767 deaths (not including deaths from complications caused by AD) in 2013 [1]. There are over 5 million individuals over the age of 65 living with AD today, and the estimated prevalence is expected to range from 11 million to 16 million by 2050 [1]. Furthermore, estimates from Medicare data suggests that one in every three seniors dies with Alzheimer's disease or another neurodegenerative disease [2,3].

In 2015, an American develops AD every 67 seconds. In 2050, an American will develop the disease every 33 seconds [1]. The total annual payments for health care, long-term care, and hospice care for individuals with AD and other dementias are estimated to increase from $226 billion in 2015 to more than $1 trillion in 2050 (both metrics are in 2015 dollars). This growth in health care payments includes a five-fold increase in government spending under Medicare and Medicaid and approximately five-fold increase in out-of-pocket spending [1].

Furthermore, deaths from Alzheimer's disease increased 71% between 2000 and 2013, while deaths from other major diseases such as heart disease (the number one cause of death in the U.S.), stroke, and prostate cancer decreased by 14%, 23%, and 11%, respectively [1]. Currently, there is no treatment to prevent, slow the progression of, or cure Alzheimer's disease. The prevalence, mortality, impact on family members/caregivers, and cost to society combined make this one of the gravest worldwide human health problems of our time.

In order to find treatments that prevent, slow the progression of, or cure Alzheimer's disease, we need to diagnose the presence of AD reliably. In order to diagnose AD reliably, we need tools to understand the pathophysiology of the disease and to be able to evaluate and monitor the progression of the disease.

To evaluate a possible neurodegenerative condition, neuroimaging, such as a Magnetic Resonance (MR) Images or Computed Tomography (CT) scans, is commonly performed to noninvasively observe structural atrophy patterns associated with such degenerative diseases. The current standard in the radiological assessment of structural information of brain images is to make a visual assessment such as "mild age-appropriate atrophy". This assessment is qualitative and therefore, highly subjective. The subtle changes in anatomy cannot be identified by broad, subjective terms such as "mild" atrophy. Furthermore, the large changes in structure, due to normal aging, present concomitantly with the structural changes due to disease, which confounds the diagnosis of neurodegenerative diseases. Therefore, we have developed tools that summarize and quantify changes in cerebral cortical shape on a global-, lobar-, regional-level. We have applied these tools to characterize normal aging across the adult human lifespan to establish a baseline of cortical shape change with normal aging. Because these tools can be applied for individual assessment, achieving our goals could have a significant clinical impact by aiding to not only understand age-appropriate changes but also, in the future, to dissociate structural changes associated with aging from those caused by dementing neurodegenerative disorders. An accurate, practical objective summary measure of the brain physiology, and subsequently pathology, would augment current subjective visual interpretation of structural magnetic resonance images.

1.2 Summary of Innovation and Overview of Forthcoming Chapters

Chapter 2 provides background information on fractal dimension, its applications and computation methods of global and local fractal dimension, for understanding the studies described in the subsequent chapters.

The methodological aspects that make this research unusually innovative go hand-in-hand with the chapters in this dissertation and have been outlined below.

1) The use of global fractal dimension as an integrative marker of cerebral cortical shape to quantitatively characterize the age-related changes in the shape of cerebral cortex from age 20 to 89 (Chapter 3).
2) The construction of age-weighted diffeomorphic atlases per age-group (half-decade and decade) from age 20 to 89 to account for the intra-age group variability to improve the sensitivity and specificity of the shape analysis (Chapter 4).
3) The use of vector energy to quantify the variability and the difference in shape of the cerebral cortex between each decade and half-decade from age 20 to 89 (Chapter 4).
4) The development of novel techniques to create global fractal dimension-weighted diffeomorphic atlases to improve the shape analysis (Chapter 4).

5) The use of local fractal dimension as a marker of cerebral cortical shape to quantitatively characterize the lobar and regional spatiotemporal changes in the shape of cerebral cortex with normal aging from age 20 to 89 (Chapter 5).

6) The development of novel techniques to apply diffeomorphic atlasing methodology to voxel-based cortico-fractal surfaces to characterize regional spatiotemporal changes in the shape of cerebral cortex (Chapter 6).

1.3 References

[1] "2015 Alzheimer"s disease facts and figures," Alzheimer's & Dementia, vol. 11, no. 3, pp. 332-384, 2015.

[2] J. Bynum, "Tabulations based on data from the National 20% Sample Medicare Fee-for-Service Beneficiaries for 2009," Unpublished raw data, 2011.

[3] J. Bynum, "Unpublished tabulations based on data from the Medicare Current Beneficiary Survey for 2008," Unpublished raw data, 2011.

CHAPTER 2

BACKGROUND

2.1 Fractal Dimension, a Measure of Cerebral Cortical Shape Complexity, as a Neuroimaging Biomarker

The human cerebral cortex undergoes numerous structural changes over the lifespan. Even in healthy adults with a normal performance with standard neuropsychologic screening measures, there are significant age-related decreases noted in regional brain volumes and cortical thickness patterns [1-3]. In Alzheimer's disease, the loss of neurons and subsequent axonal degeneration leads to cerebral atrophy; the structural effects on the cerebral cortex include widening of sulci and thinning of the cortical ribbon [4]. Several cross-sectional imaging studies have quantified volumetric changes in cortical and sub-cortical structures as a function of healthy aging as well as pathological processes such as hypertension, cerebrovascular disease, and neurodegenerative diseases. However, the assessment of cerebral cortical shape has been less well explored. Analysis of shape is a complementary approach to volumetric analysis, which quantifies other

important structural properties beyond the standard measurement of area.

Neuroimaging studies in recent years have highlighted the numerous important properties of the human cerebral cortex. One of the more interesting characteristics of the cortex is that it displays fractal properties (i.e., statistical similarity in shape) over a range of spatial scales [5-11]. Fractal dimension analysis was first made popular by a series of works by Benoit Mandelbrot in the late 1970s and early 1980s [12,13]. These analytic techniques can capture very complicated structures using relatively simple computational algorithms. Scientists have used fractal analysis for many years to quantify geologic phenomena such as decay of coastlines, analyzing cracks in crystal structure, botanical simulation, and atmospheric modeling [14]. It had been proposed that these same principles could be used to quantify the spatial properties of the surface of the brain.

Studies using anatomical data from either gross specimens [15] or magnetic resonance images [9-11,16] have demonstrated that the human cerebral cortex exhibits fractal properties, such as being statistically self-similar (magnification of smaller scale structure resembles the large-scale structure). The complexity of the cerebral cortex can be quantified by a numerical value known as fractal dimension [12,13]. The underlying cerebral white matter, as well as the cerebellum and supporting white matter tracts, are amenable to study using fractal approaches [17-21].

2.2 Validating the Clinical Need for a Structural Neuroimaging Biomarker

Cerebral cortical shape complexity assessment is important because it provides a clinically useful and applicable method to quantify shape change. The numerical value of fractal dimension has a definite visual correlate, as seen in Figure 2.1. Cortical complexity is otherwise difficult to reliably assess in clinical practice. The current standard in the radiological assessment of brain images is to make a subjective visual assessment such as "mild age-appropriate atrophy". This type of assessment is very limited because the evaluation varies significantly between individuals, there is no definition of the terms (what does "mild" mean), and because subtle changes cannot be identified using such broad terms. Quantification of these age-related changes will enable currently subjective measures of "age-appropriate" atrophy to be objectively quantified, and thus improve our understanding of atrophic changes on an individual basis.

2.3 Advantages of Fractal Dimension Analysis

Currently, there exist several techniques for assessment of cerebral morphology, such as manual ROI-based volumetric approaches [22], hippocampal shape analysis [23], voxel-based morphometry [24,25], cortical pattern matching [26,27], brain boundary shift integral [28], cortical thickness [29-31], and regional cortical segmentation [32]. These techniques

can reliably differentiate patients with AD from controls by demonstrating decreases in brain volumes [33-36]. But volumetric characterization is one of many aspects of human anatomical structure and some of these techniques are overly simplistic. Additional information not available by volumetric analysis may be gained using other analysis techniques, such as shape analysis [37]. Shape characterization has proven be a useful method for identifying clinically relevant information on neuroimaging scans [23,36,38].

The folding of the human cerebral cortex reflects the complex underlying architectural features that evolve during brain development and degeneration including neuronal density, synaptic proliferation and loss, and gliosis. The shape complexity of cerebral cortical folding changes with normal aging as well as with neurodegenerative diseases and cortical properties such as gyrification index, cortical thickness, and sulcal depth are altered. The fractal properties of the cerebral cortex arise secondary to folding [15]; diseases that alter cortical properties, such as gyrification index, cortical thickness, and sulcal depth, will become a natural target for fractal analysis. Fractal analysis integrates information over a range of spatial scales (two orders of magnitude from 0.5 mm to ~30 mm) [24]. The range over which the fractal analysis is valid can be determined by measuring the consistency (scale invariance) in the cube count/size slope [20]. Given the range, this unique approach to shape analysis can integrate several aspects of structural change associated with disease, i.e., both subtle changes in cortical thickness

associated with synaptic and neuronal loss as well as larger scale changes in the width and depth of sulci. Also, fractal dimension is a direct measure of gray matter atrophy and underlying cytoarchitectural changes, as compared to other shape metrics derived from secondary image processing methods [39,40]. Therefore, fractal dimension provides a quantitative, aggregate measure of shape complexity describing this multiscale folding of the human cerebral cortex from neuroradiological scans.

Furthermore, fractal dimension analysis has been proven to be complementary, and in some cases, a more advantageous methodology, to several existing methodologies, such as volumetric studies [23,20,41], voxel-based morphometry [19,42-45], traditional MR morphometric analysis [46], and cortical thickness and gyrification [45,47].

2.4 Computation of Global Fractal Dimension

Fractal dimension analysis has been used to study epilepsy [16], schizophrenia [38,46,48,49], and cortical development [50,51], but our lab was the first to demonstrate practical application in AD [47,42]. We have demonstrated that changes in the fractal dimension in the cortex occur in Alzheimer's disease using 2D slicing methods [47]. Furthermore, we have also demonstrated that the fractal analysis method is more effective when applied to the entire cortical ribbon instead of just the inner or outer surfaces, and that the cortical ribbon does a better job of distinguishing

Alzheimer's disease from healthy controls than cortical thickness or gyrification index [42]. Additionally, the pattern of loss of cerebral cortical complexity differs between diseases reflecting selective neuronal vulnerability and/or regional disease expression. Therefore, we have written custom software to perform a global and local (voxel-wise and regional) fractal analysis and create cortico-fractal surfaces (discussed in Chapter 6) in the original 3D image space.

There are several approaches for computing the fractal dimension of objects, such as caliper methods [13,52,53], box-counting algorithms [13,54], dilation methods [55], and spatial frequency analysis [9]. We selected a box-counting algorithm because of the simplicity of implementation as well as for comparison to other studies that use this method to examine fractal properties of the human brain [7,10,11,16,17,18,20,21].

The fractal dimension (FD) of the cortical surfaces was computed using a custom software program called Cortical Complexity Calculator (C^3), which is based on a 3D cube-counting algorithm. This algorithm has been described by [13,54], and used by several previous investigators [7,8]. Furthermore, this algorithm has been shown to be a robust and accurate method of computing cortical complexity [8]. The implementation of this algorithm that has been applied for this study is very similar to [8].

C^3 uses a 3D cube-counting algorithm, which tiles the tessellated triangles (~200,000 per surface per hemisphere) with cubes of varying sizes.

This approach is derived from the Minkowski-Bouligand dimension with an extrapolation using 3D cubes instead of 2D boxes. The cube count for each hemisphere covers the entire cortical ribbon, including the pial surface, gray-white surface, and all necessary intermediate surfaces (temporary 3D meshes spatially contained between the pial surface and gray-white surface. Intermediate surfaces can be dynamically generated as needed to create a full model of the entire cortical ribbon, as described in a previous study [42]. The intersection of each triangle (including the edges) with a cube matrix covering the entire brain is computed using standard geometry. Each cube is counted only once, resulting in a cube count of the total number of intersections. The cube size is then changed, and the intersection computation is repeated. The fractal dimension of an object, also known as the Hausdorf–Besikovich dimension, is computed as the change in the log of the cube count divided by the change in the log of the cube size (see Equation (2.1)).

$$FD = -\frac{\Delta \log(cube\ count)}{\Delta \log(cube\ size)} \tag{2.1}$$

The version of C3 used in this study was written on Mac OS X (10.5) using the XCode environment in Objective C with graphic implementation using OpenGL.

2.5 Computation of Local Fractal Dimension

Most studies of the fractal properties of the cerebral cortex have focused on computing whole-brain measures (i.e., generating one number which summarizes the entire hemisphere). It is well established that aging has differential effects on the cerebral cortex, with some regions being more selectively prone to age-related atrophy and this is true for progressive neurodegenerative diseases, such as Alzheimer's disease, as well [1-3,56].

Furthermore, the local pattern of cortical complexity loss with aging likely differs from alterations associated with neurodegenerative disease such as Alzheimer's disease or Frontotemporal dementia. Thus, a local analysis of the cortical complexity of regions more prone to change will likely increase the sensitivity and specificity of the analysis.

To compute local values of fractal dimension, the process of cube-counting was performed at every voxel that was labeled as belonging to the cerebral cortex. Instead of including the entire cortex in the counting, only those voxels located within a cubic region of 30mm were included. For details of this process, see [57].

2.6 References

[1] K. Walhovd, L. Westlye, I. Amlien, T. Espeseth, I. Reinvang, N. Raz, I. Agartz, D. Salat, D. Greve, B. Fischl, A. Dale and A. Fjell, "Consistent neuroanatomical age-related volume differences across multiple samples," Neurobiology of Aging, vol. 32, no. 5, pp. 916-932, 2011.

[2] N. Raz, "Regional brain changes in aging healthy adults: general trends, individual differences and modifiers," Cerebral Cortex, vol. 15, no. 11, pp. 1676-1689, 2005.

[3] N. Raz, P. Ghisletta, K. Rodrigue, K. Kennedy and U. Lindenberger, "Trajectories of brain aging in middle-aged and older adults: regional and individual differences," NeuroImage, vol. 51, no. 2, pp. 501-511, 2010.

[4] P. Thompson, "Tracking Alzheimer's disease," Annals of the New York Academy of Sciences 1097, no. 1, pp. 183-214, 2007.

[5] E. Bullmore, M. Brammer, I. Harvey, R. Persaud, R. Murray and M. Ron, "Fractal analysis of the boundary between white matter and cerebral cortex in magnetic resonance images: a controlled study of schizophrenic and manic-depressive patients," Psychological Medicine, vol. 24, no. 03, p. 771, 1994.

[6] S. Free, S. Sisodiya, M. Cook, D. Fish and S. Shorvon, "Three-dimensional fractal analysis of the white matter surface from magnetic resonance images of the human brain," Cerebral Cortex, vol. 6, no. 6, pp. 830-836, 1996.

[7] K. Im, J. Lee, U. Yoon, Y. Shin, S. Hong, I. Kim, J. Kwon and S. Kim, "Fractal dimension in human cortical surface: multiple regression analysis with cortical thickness, sulcal depth, and folding area," Human Brain Mapping, vol. 27, no. 12, pp. 994-1003, 2006.

[8] J. Jiang, W. Zhu, F. Shi, Y. Zhang, L. Lin and T. Jiang, "A robust and accurate algorithm for estimating the complexity of the cortical surface," Journal of Neuroscience Methods, vol. 172, no. 1, pp. 122-130, 2008.

[9] V. Kiselev, K. Hahn and D. Auer, "Is the brain cortex a fractal?," NeuroImage, vol. 20, no. 3, pp. 1765-1774, 2003.

[10] J. Lee, U. Yoon, J. Kim, I. Kim, D. Lee, J. Kwon and S. Kim, "Analysis of the hemispheric asymmetry using fractal dimension of a skeletonized cerebral surface," IEEE Transactions on Biomedical Engineering, vol. 51, no. 8, pp. 1494-1498, 2004.

[11] S. Majumdar and R. Prasad, "The fractal dimension of cerebral surfaces using magnetic resonance images," Computers in Physics, vol. 2, no. 6, pp. 69, 1988.

[12] D. Bresson and B. Mandelbrot, “Fractals: form, chance, and dimension,” Leonardo, vol. 12, no. 3, pp. 248, 1979.

[13] B. Mandelbrot, The fractal geometry of nature. New York: W.H. Freeman, 1983.

[14] D.E. Herbert, P. Croft, “Chaos and the changing nature of science and medicine: an introduction by Donald E. Herbert,” Med. Phys., vol. 24, no. 8, p. 1336, 1997.

[15] M.A. Hofman, “The fractal geometry of convoluted brains. Journal fur Hirnforschung, vol 32, no. 1, pp. 103-111, 1990.

[16] M. Cook, S. Free, M. Manford, D. Fish, S. Shorvon and J. Stevens, “Fractal description of cerebral cortical patterns in frontal lobe epilepsy,” European Neurology, vol. 35, no. 6, pp. 327-335, 1995.

[17] F. Esteban, J. Sepulcre, N. de Mendizábal, J. Goñi, J. Navas, J. de Miras, B. Bejarano, J. Masdeu and P. Villoslada, “Fractal dimension and white matter changes in multiple sclerosis,” NeuroImage, vol. 36, no. 3, pp. 543-549, 2007.

[18] J. Liu, L. Zhang and G. Yue, “Fractal dimension in human cerebellum measured by magnetic resonance imaging,” Biophysical Journal, vol. 85, no. 6, pp. 4041-4046, 2003.

[19] Y. Wu, K. Shyu, C. Jao, Z. Wang, B. Soong, H. Wu and P. Wang, “Fractal dimension analysis for quantifying cerebellar morphological change of multiple system atrophy of the cerebellar type (MSA-C),” NeuroImage, vol. 49, no. 1, pp. 539-551, 2010.

[20] L. Zhang, D. Dean, J. Liu, V. Sahgal, X. Wang and G. Yue, “Quantifying degeneration of white matter in normal aging using fractal dimension,” Neurobiology of Aging, vol. 28, no. 10, pp. 1543-1555, 2007.

[21] L. Zhang, J. Liu, D. Dean, V. Sahgal and G. Yue, “A three-dimensional fractal analysis method for quantifying white matter structure in human brain,” Journal of Neuroscience Methods, vol. 150, no. 2, pp. 242-253, 2006.

[22] C. Jack, M. Shiung, S. Weigand, P. O”Brien, J. Gunter, B. Boeve, D. Knopman, G. Smith, R. Ivnik, E. Tangalos and R. Petersen, “Brain atrophy rates predict subsequent clinical conversion in normal elderly and amnestic MCI,” Neurology, vol. 65, no. 8, pp. 1227-1231, 2005.

[23] J. Csernansky, L. Wang, J. Swank, J. Miller, M. Gado, D. McKeel, M. Miller and J. Morris, "Preclinical detection of Alzheimer"s disease: hippocampal shape and volume predict dementia onset in the elderly," NeuroImage, vol. 25, no. 3, pp. 783-792, 2005.

[24] J. Ashburner and K. Friston, "Voxel-based morphometry—the methods," NeuroImage, vol. 11, no. 6, pp. 805-821, 2000.

[25] C. Good, I. Johnsrude, J. Ashburner, R. Henson, K. Friston and R. Frackowiak, "A voxel-based morphometric study of ageing in 465 normal adult human brains," NeuroImage, vol. 14, no. 1, pp. 21-36, 2001.

[26] P. Thompson, "Cortical variability and asymmetry in normal aging and Alzheimer"s disease," Cerebral Cortex, vol. 8, no. 6, pp. 492-509, 1998.

[27] P. Thompson, M. Mega, R. Woods, C. Zoumalan, C. Lindshield, R. Blanton, J. Moussai, C. Holmes, J. Cummings and A. Toga, "Cortical change in Alzheimer"s disease detected with a disease-specific population-based brain atlas," Cerebral Cortex, vol. 11, no. 1, pp. 1-16, 2001.

[28] N. Fox, S. Cousens, R. Scahill, R. Harvey and M. Rossor, "Using serial registered brain magnetic resonance imaging to measure disease progression in Alzheimer disease," Arch Neurol, vol. 57, no. 3, p. 339, 2000.

[29] B. Fischl and A. Dale, "Measuring the thickness of the human cerebral cortex from magnetic resonance images," Proceedings of the National Academy of Sciences, vol. 97, no. 20, pp. 11050-11055, 2000.

[30] A. Fjell, K. Walhovd, I. Reinvang, A. Lundervold, D. Salat, B. Quinn, B. Fischl and A. Dale, "Selective increase of cortical thickness in high-performing elderly—structural indices of optimal cognitive aging," NeuroImage, vol. 29, no. 3, pp. 984-994, 2006.

[31] K. Walhovd, A. Fjell, I. Reinvang, A. Lundervold, A. Dale, B. Quinn, D. Salat, N. Makris and B. Fischl, "Neuroanatomical aging: universal but not uniform," Neurobiology of Aging, vol. 26, no. 9, pp. 1279-1282, 2005.

[32] J. Rademacher, V. Caviness, H. Steinmetz and A. Galaburda, "Topographical variation of the human primary cortices: implications for neuroimaging, brain mapping, and neurobiology," Cerebral Cortex,

vol. 3, no. 4, pp. 313-329, 1993.

[33] J. Csernansky, L. Wang, J. Miller, J. Galvin and J. Morris, "Neuroanatomical predictors of response to donepezil therapy in patients with dementia," Arch Neurol, vol. 62, no. 11, p. 1718, 2005.

[34] B. Dickerson, D. Salat, D. Greve, E. Chua, E. Rand-Giovannetti, D. Rentz, L. Bertram, K. Mullin, R. Tanzi, D. Blacker, M. Albert and R. Sperling, "Increased hippocampal activation in mild cognitive impairment compared to normal aging and AD," Neurology, vol. 65, no. 3, pp. 404-411, 2005.

[35] B. Dickerson and R. Sperling, "Neuroimaging biomarkers for clinical trials of disease-modifying therapies in Alzheimer"s disease," Neurotherapeutics, vol. 2, no. 2, pp. 348-360, 2005.

[36] L. Wang, J. Swank, I. Glick, M. Gado, M. Miller, J. Morris and J. Csernansky, "Changes in hippocampal volume and shape across time distinguish dementia of the Alzheimer type from healthy aging⋆," NeuroImage, vol. 20, no. 2, pp. 667-682, 2003.

[37] G. Gerig, M. Styner, M. E. Shenton, J. A. Lieberman, "Shape versus size: Improved understanding of the morphology of brain structures," in Proc. In Medical Image Computing and Computer-Assisted Intervention, pp. 24-32, 2001.

[38] M. F. Casanova, "Quantitative shape analysis of the temporal and prefrontal lobes of schizophrenic patients: a magnetic resonance image study," JNP, vol. 2, no. 4, pp. 363-372, 1990.

[39] L. Regeur, "Increasing loss of brain tissue with increasing dementia: a stereological study of post-mortem brains from elderly females," European Journal of Neurology, vol. 7, no. 1, pp. 47-54, 2000.

[40] V. Singh, H. Chertkow, J. Lerch, A. Evans, A. Dorr and N. Kabani, "Spatial patterns of cortical thinning in mild cognitive impairment and Alzheimer"s disease," Brain, vol. 129, no. 11, pp. 2885-2893, 2006.

[41] L. Zhang, A. Butler, C. Sun, V. Sahgal, G. Wittenberg and G. Yue, "Fractal dimension assessment of brain white matter structural complexity post stroke in relation to upper-extremity motor function," Brain Research, vol. 1228, pp. 229-240, 2008.

[42] R. King, B. Brown, M. Hwang, T. Jeon and A. George, "Fractal dimension analysis of the cortical ribbon in mild Alzheimer"s disease," NeuroImage, vol. 53, no. 2, pp. 471-479, 2010.

[43] V. Rajagopalan, Z. Liu, D. Allexandre, L. Zhang, X. Wang, E. Pioro and G. Yue, "Brain white matter shape changes in Amyotrophic Lateral Sclerosis (ALS): A fractal dimension study," PLoS ONE, vol. 8, no. 9, pp. e73614, 2013.

[44] F. Esteban, J. Sepulcre, J. de Miras, J. Navas, N. de Mendizábal, J. Goñi, J. Quesada, B. Bejarano and P. Villoslada, "Fractal dimension analysis of grey matter in multiple sclerosis," Journal of the Neurological Sciences, vol. 282, no. 1-2, pp. 67-71, 2009.

[45] J. Lin, N. Salamon, A. Lee, R. Dutton, J. Geaga, K. Hayashi, E. Luders, A. Toga, J. Engel and P. Thompson, "Reduced neocortical thickness and complexity mapped in mesial temporal lobe epilepsy with hippocampal sclerosis," Cerebral Cortex, vol. 17, no. 9, pp. 2007-2018, 2006.

[46] T. Ha, U. Yoon, K. Lee, Y. Shin, J. Lee, I. Kim, K. Ha, S. Kim and J. Kwon, "Fractal dimension of cerebral cortical surface in schizophrenia and obsessive–compulsive disorder," Neuroscience Letters, vol. 384, no. 1-2, pp. 172-176, 2005.

[47] R. King, A. George, T. Jeon, L. Hynan, T. Youn, D. Kennedy and B. Dickerson, "Characterization of atrophic changes in the cerebral cortex using fractal dimensional analysis," Brain Imaging and Behavior, vol. 3, no. 2, pp. 154-166, 2009.

[48] M. Casanova, D. Daniel, T. Goldberg, R. Suddath and D. Weinberger, "Shape analysis of the middle cranial fossa of schizophrenic patients: A computerized tomographic study," Schizophrenia Research, vol. 2, no. 1-2, p. 133, 1989.

[49] A. Sandu, I. Rasmussen, A. Lundervold, F. Kreuder, G. Neckelmann, K. Hugdahl and K. Specht, "Fractal dimension analysis of MR images reveals grey matter structure irregularities in schizophrenia," Computerized Medical Imaging and Graphics, vol. 32, no. 2, pp. 150-158, 2008.

[50] P. Thompson, "Abnormal cortical complexity and thickness profiles mapped in Williams Syndrome," Journal of Neuroscience, vol. 25, no. 16, pp. 4146-4158, 2005.

[51] Y. Wu, K. Shyu, T. Chen and W. Guo, "Using three-dimensional fractal dimension to analyze the complexity of fetal cortical surface from magnetic resonance images," Nonlinear Dynamics, vol. 58, no. 4, pp. 745-752, 2009.

[52] T. Smith, W. Marks, G. Lange, W. Sheriff and E. Neale, "A fractal analysis of cell images," Journal of Neuroscience Methods, vol. 27, no. 2, pp. 173-180, 1989.

[53] H. Takayasu, Fractals in the physical sciences. Manchester: Manchester University Press, 1990.

[54] F. Caserta, W. Eldred, E. Fernandez, R. Hausman, L. Stanford, S. Bulderev, S. Schwarzer and H. Stanley, "Determination of fractal dimension of physiologically characterized neurons in two and three dimensions," Journal of Neuroscience Methods, vol. 56, no. 2, pp. 133-144, 1995.

[55] E. Fernández and H. Jelinek, "Use of fractal theory in neuroscience: methods, advantages, and potential problems," Methods, vol. 24, no. 4, pp. 309-321, 2001.

[56] K. Kennedy, K. Erickson, K. Rodrigue, M. Voss, S. Colcombe, A. Kramer, J. Acker and N. Raz, "Age-related differences in regional brain volumes: A comparison of optimized voxel-based morphometry to manual volumetry," Neurobiology of Aging, vol. 30, no. 10, pp. 1657-1676, 2009.

[57] R. King, "Computation of local fractal dimension values of the human cerebral cortex," AM, vol. 05, no. 12, pp. 1733-1740, 2014.

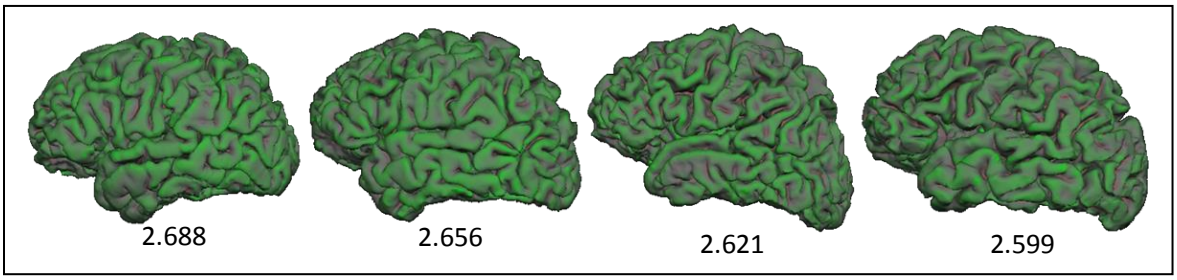

Figure 2.1 Visual correlates of cortical fractal dimension. Shown are views of the pial surface of the left hemisphere for 4 subjects with a range of cortical complexity. Local curvature is mapped to the color scale (green = highest curvature, gray = lowest curvature) to allow better visualization of the 3D properties. Visually, the decreased complexity is associated with widened sulci and smaller gyri. All of these subjects had normal cognition.

CHAPTER 3

FRACTAL ANALYSIS OF THE CEREBRAL CORTICAL RIBBON ACROSS THE ADULT HUMAN LIFESPAN

3.1 Abstract

Fractal dimension analysis of high-resolution magnetic resonance images is a method for quantifying the complexity of the human cerebral cortex. In order to use cortical fractal dimension as a biomarker for age-related diseases, it is critical to establish the influence of aging on cortical complexity. The purpose of this paper is to examine age-related differences in cortical complexity across the adult lifespan in a large cross-sectional cohort of well-characterized, cognitively normal, healthy adults.

MR images of the brain from 301 subjects in the Dallas Lifespan Brain Study (age range 20-89, ~43 per decade) were analyzed using FreeSurfer to segment volumetric parameters and generate 3D surface models of the cortex. The global cortical fractal dimension was computed from the surface models using customized cube-counting software. Additionally, the volumes of subcortical and cortical regions were calculated along with cortical

thickness, surface area, and gyrification index measures.

Global fractal dimension of the cortex decreases precipitously with age ($r = -0.801$, $R^2 = 0.642$). Significant differences ($p < 0.05$) in average cortical complexity occur between all successive decades except for between the 40s and 50s ($p = 0.08$). Cortical thickness had the strongest age-related effect ($r = -0.662$, $R^2 = 0.438$), followed by gyrification index ($r = -0.546$, $R^2 = 0.298$) and brain volume ($r = -0.455$, $R^2 = 0.298$). Cortical surface area was weakly correlated with age ($r = -.296$, $R^2 = 0.087$). Cortical thickness and gyrification index were the strongest drivers of cortical fractal dimension.

Significant alterations in the shape of the cerebral cortex occur throughout the adult lifespan, and these changes can be quantified using global cortical fractal dimension. Now that the normal range of age-related complexity values have been identified, this tool can be used to identify structural changes not associated with normal aging.

3.2 Introduction

The human cerebral cortex undergoes a number of structural changes over the lifespan. Even in healthy adults with a normal performance on standard neuropsychologic screening measures, there are significant age-related decreases noted in regional brain volumes and cortical thickness patterns [1-3]. Many cross-sectional imaging studies [4-6] have quantified volumetric changes in cortical and sub-cortical structures as a function of

healthy aging as well as in pathological processes such as hypertension, cerebrovascular disease, and neurodegenerative diseases [7].

While cortical volumetric properties have been well characterized, the assessment of cortical shape has been less well explored. Analysis of shape is a complementary approach to volumetric analysis, which quantifies other important structural properties beyond the standard measurement of area. In particular, the folding of the cerebral cortex creates shapes that are statistically similar over a range of spatial scales. The complexity of these folding patterns can be characterized using a measure known as fractal dimension. Studies using anatomical data from either tissue specimens and magnetic resonance images have demonstrated that the human cerebral cortex exhibits fractal properties [8-15].

Fractal dimension analysis was first made popular by a series of works by Benoit Mandelbrot in the late 1970s and early 1980s [16,17]. These analytic techniques can capture very complicated structures using relatively simple computational algorithms [18]. Mathematically created fractal objects exhibit a property called "self-similarity", which means that magnification of smaller scale features exactly duplicate a larger scale structure. This approach has been applied to the analysis of brain structure several times in recent years. The underlying cerebral white matter, as well as the cerebellum and supporting white matter tracts, are amenable to study using fractal approaches [19-23]. The approach has been used to study epilepsy [24],

schizophrenia [25-28], cortical development [29,30], and Alzheimer's disease [31,32].

Recent methodological advancements in cortical fractal analysis include a technique to analyze the entire cortical ribbon as derived from 3D tessellated polygon models of cortex segmented from high-resolution high-contrast T1 weighted images [32]. This technique offers significant improvements over using models of the pial (outer cortical) surface or gray-white (inner cortical) surface in terms of differentiating healthy aging from neurodegenerative processes on a group-comparison basis. However, the effects of aging on the complexity of the cortical ribbon have not yet been explored. The purpose of this paper is to examine age-related differences in cortical complexity across the adult lifespan in a large cross-sectional cohort of cognitively normal adults. These complexity differences will be also compared to currently used volumetric assessments of the cerebral cortex (thickness, volume, surface area, and gyrification index).

3.3 Methodology

3.3.1 Participants

Participants consisted of 301 individuals aged 20-88 (mean 52.8 ± 19.6 years; uniform age distribution with ~43 subjects per decade; 192 women, 109 men) from the Dallas Lifespan Brain Study (DLBS). DLBS is a large-scale longitudinal research project designed to characterize neural and cognitive

aging across the adult lifespan from age 20 to 89. These participants were recruited through media advertisements and flyers and underwent health history screening via a health questionnaire as well as telephone and personal interviews. All participants were screened against cardiovascular, neurological, and psychiatric disorders, head injury with loss of consciousness > 10 min, and drug/alcohol abuse. Additional exclusion criteria for our study were irregularities in the MR image and inability to produce cortical surfaces via the FreeSurfer pipeline (discussed below). Participants were native English speakers and strongly right-handed (on the Edinburgh Handedness Questionnaire [33]. The participants were well educated (mean 16.58 ± 2.66 years) and scored highly (28.31 ± 1.31) on the Mini Mental State Examination (MMSE; [34]). All participants provided written informed consent and were debriefed in accord with university human investigations committee guidelines.

3.3.2 MRI Acquisition

All participants were scanned on a single 3T Philips Achieva scanner equipped with an 8-channel head coil. High-resolution anatomical images were collected with a T1-weighted MP-RAGE sequence with 160 sagittal slices, 1×1×1mm^3 voxel; 204×256×160 matrix, TR=8.1ms, TE=3.7ms, flip-angle=12°. See Table 3.1 for a demographic summary of the subjects.

3.3.3 MRI Processing

Segmentation of the brain images was performed using a semiautomated segmentation software suite called FreeSurfer (version 4.4.0, Athinoula A. Martinos Center for Biomedical Imaging, Massachusetts General Hospital, Boston). FreeSurfer contains a set of tools for analysis and visualization of structural and functional brain imaging data. FreeSurfer has been described in detail in prior publications [35-43].

FreeSurfer was also used to generate three-dimensional tessellated polygon models of the inner (gray-white) and outer (pial) cortical surfaces. Preliminary segmentation of the gray matter from the white matter was generated based on intensity differences and geometric structure differences in the gray/white junction [44]. The pial surface was generated using outward deformation of the gray/white surface with a second-order smoothness constraint [36,44]. The smoothness constraint allowed the pial surface to be extended into otherwise ambiguous areas. The resulting surfaces have sub-voxel accuracy.

Manual editing was performed to correct for errors in the gray-white boundary (e.g., subcortical T1 hypointense regions improperly included as cortex or white matter boundaries incorrectly drawn due to improper intensity normalization) and the pial boundary (e.g., meningeal dural tissue not fully removed by the skull-stripping procedure).

The fractal dimension (FD) of the cortical ribbon was computed using a custom software program called the Cortical Complexity Calculator, which is based on a 3D cube-counting algorithm (described in Chapter 2). The software directly imports the FreeSurfer surface models to perform the complexity analysis in native space.

3.3.4 Data Analysis

A mean FD value was extracted for each subject and the values of cortical fractal dimension between successive decade-wide cohorts were compared using a Student's t-test (one-tailed, $\alpha < 0.05$ considered significant) to determine between which decades FD differences were most apparent. To determine whether there are significant differences in the variance of fractal dimension as a function of age, an F-statistic was computed to compare the variance across decades. Critical values were determined for each decade pairing at the $\alpha = 0.05$ significance level.

To examine relationships between cortical fractal dimension and population demographic factors, we performed a general linear model (GLM) using gender, age, education, MMSE scores, and intracranial volume (ICV) as predictive factors. To explore relationships between cortical fractal dimension and other commonly used measures of brain structure, values for average cortical thickness (CT), total segmented brain volume (BV), total cortical surface area (SA), and gyrification index (GI, a ratio of the total cortical

surface area to the surface area of a tightly-wrapping smoothed cortical surface) were extracted from the FreeSurfer data files. A GLM was created (using SPSS Statistics, IBM, version 21.0.0.0) entering CT, BV, SA, GI, and age as independent variables to determine which structural factors best predicted FD.

3.4 Results

3.4.1 Frequency Distribution Plot of DLBS Data

The frequency distribution plot of the 301 cognitively normal subjects in the Dallas Lifespan Brain study database has been created (Figure 3.1).

We have presented two subjects (MR image and 3D surface model generated by FreeSurfer for each subject) on either side of the spectrum, one which is of a 78-year-old subject with a FD of 2.599 (bottom) and one which is of a 24-year-old subject with a FD of 2.688 (top) to visualize the differences in shape of the cerebral cortex across the spectrum.

3.4.2 Cortical Ribbon Complexity Differences Across the Lifespan

On average, we found that the fractal dimension of the cortex decreased with age, and there was a strong correlation between the two, with age alone accounting for 64% of the variance in cortical complexity (Pearson r = -0.801, R^2 = 0.642). Whole brain fractal dimension as a function of age is

shown in Figure 3.2 and summarized in Table 3.2 by decade. The most significant age-related differences in cortical complexity occurred earlier in the adult lifespan. The difference between the 20s and 30s and between the 30s and 40s were highly significant ($p < 0.0001$). In contrast, no statistically significant decrease in average cortical fractal dimension was observed between the 40s and 50s, ($p = 0.08$), where the smallest absolute difference in average FD was seen. Significant differences were again seen between older cohorts (60s, 70s, and 80s, $p < 0.02$). All cohorts separated by at least 20 years differed significantly ($p < 0.0001$ for all pairwise t-tests).

The degree of significance was smaller among older cohorts than younger cohorts, possibly due to the increased variability observed in the older cohorts. The variance for each decade was compared using F-test for homoscedastisticy between decades. We found the degree of variability in cortical complexity increases with age, with significant difference in variance observed between the youngest and oldest cohorts (F-Test $p < 0.05$ for 20s vs. 80s, 30s vs. 70s, 30s vs. 80s, and 40s vs. 80s; see Table 3.2).

3.4.3 Cortical Ribbon Complexity and Demographic Factors

Zero-order Pearson correlations indicated that cortical fractal dimension was significantly associated with age ($R^2 = 0.642$, $p < 0.001$), years of education ($R^2 = 0.021$, $p = 0.047$), MMSE ($R^2 = 0.105$, $p < 0.001$), but not with

ICV (R^2 = 0.006, p = 0.18) or gender (average FD for Females = 2.649, Males 2.648, p = 0.477). To consider the combined effects of these demographic characteristics, we conducted a GLM with age, gender, MMSE, education, and ICV as predictors of FD. We found a significant effect of age (F [1, 294]= 440.85, p < 0.001) and education (F [1, 294]= 3.98, p = 0.047) on FD, where older age and fewer years of education were associated with less cortical complexity. We found no significant effect on global cortical fractal dimension between genders (F < 1, p = 0.546), MMSE scores (F < 1, p = 0.704), or ICV in this sample (F < 1, p = 0.698) after controlling for the effects of each other.

3.4.4 Cortical Ribbon Complexity Versus Other Structural Measures of the Cortex

We also examined separately the effect of age on common volumetric properties: cortical thickness, cortical surface area, brain volume, and gyrification index. As shown in Figure 3.3, all four of these measurements demonstrated significant decreases over the adult lifespan. Of these four indices, cortical thickness had the highest correlation with age (r = -0.662), followed by gyrification index (r = -0.546) and brain volume (r = -0.455). Cortical surface area was weakly correlated with age (r = -0.296).

3.4.5 General Linear Model Incorporating Other Structural Measures of the Cortex

To consider the relative association of these structural variables with FD, a general linear model including age, thickness, gyrification index, surface area, and volume were entered as predictors of FD (see Table 3.3). Both cortical thickness ($F[1,295] = 44.4$, $p < 0.001$, $\eta = 0.28$) and gyrification index ($F[1,295] = 40.1$, $p < 0.001$, $\eta = 0.36$) were significant factors in predicting cortical fractal dimension. Note that cortical thickness and gyrification index were not strongly correlated with each other ($r = 0.226$). Intracranial Volume ($F[1,295] = -2.0$, $p = 0.31$, $\eta < 0.001$) has no predictive value for fractal dimension. Cortical surface area ($F[1,295] = -11.0$, $p < 0.001$, $\eta = 0.05$) has a small effect on predicting fractal dimension. Age ($F[1,295] = -13.0$, $p < 0.001$, $\eta = 0.03$) also has a small effect, and is no longer a strong predictor of FD once cortical thickness and gyrification index are accounted for in the model.

3.5 Discussion

To the best of our knowledge, this is the first large, cross-sectional study to report on quantitative characterization of changes in cerebral cortical complexity through the adult human lifespan for a cognitively normal population. A previous study explored cortical complexity changes across the lifespan, but had a scantily distributed population, particularly with a low

sampling of older adults (only 9 out of 93 subjects over the age of 40) [45]. The current data suggest a linear decrease in cerebral cortical complexity with age across the adult human lifespan. This study benefits from using a 3-dimensional technique that incorporates the entire thickness of the cortex when computing cerebral cortical fractal dimension [31]. Previous researchers reported both linear decreases with aging in other measurements of brain area, such as cortical thickness [54,55], and volumetric measures [56-58], as well as a structural changes that accelerate with aging using tools such as voxel-based morphometry [46,59], gray matter density [60], and volumetric measures [2,47,61-65]. We speculate that one reason that structural changes do not accelerate with aging in the population for this study is that this is a highly selected healthy research population with advantageous demographic factors (i.e., education, ethnicity, socioeconomic status, etc.), and may not represent the population at large.

Cortical fractal dimension reflects a combination of volumetric factors (cortical thickness) and spatial factors (gyrification index). The findings in this paper are consistent with studies performed on images of normal adults and subjects with Alzheimer's disease [30]. The integration of multiple aspects of brain morphometry results in fractal dimension metrics having a larger effect size than either cortical thickness or gyrification index. The fact that fractal dimension is independent of head size (intracranial volume) is expected given that fractal dimension is a scale invariant measure. This may

also explain why there is not much of a gender effect on fractal dimension.

This study identified significant age-related differences in complexity occurring in the 20s and 30s, well before subjects complain of cognitive slowing and well before typical age-related diseases such as Alzheimer's disease or recurrent microvascular insults are manifested. There are certainly still changes in synaptic connectivity occurring during this earlier period in life, and perhaps a decreasing complexity reflects more specificity in cortical wiring. The clinical significance of these differences needs further exploration.

We found an increase in variability of cortical fractal dimension with older age. This increased variability occurs despite the fact that all subjects maintained normal cognition and no subjects had a significant burden of microvascular disease (which was an exclusion criteria). Understanding the sources of this variability and the long-term clinical significance are important next steps.

It remains to be determined if age-related differences in cortical complexity are linked with the commonly observed cognitive changes in normal aging. In these data, we saw a glimpse of this possibility in a significant correlation of FD with the MMSE scores (although nonsignificant after accounting for age), suggesting that there may be neuropsychological correlates of these cortical changes that should be further explored with detailed cognitive assessments. Additionally, this method may be useful in

distinguishing normal from pathological aging. There are visual correlates to the computed fractal dimension, with decreased dimension being associated with widened sulci and thinner cortex. This technique provides a quantitative method for measuring complexity, which currently is assessed by radiologists using imprecise qualitative terms such a “mild age-appropriate atrophy”. The fractal analysis method described in this paper can replace such qualitative terms with a quantitative and precise measure.

Another useful extension of the approach used in this paper is to enable a regional analysis of cortical fractal dimension (which could be analyzed locally at thousands of locations across the cortex) rather than generating a single number that summarizes the complexity of the entire cerebrum. It is well established that aging has differential effects on the cerebral cortex, with some regions being more selectively prone to age-related atrophy [58]. Furthermore, the local pattern of cortical complexity loss with aging likely differs from alterations associated with neurodegenerative disease such as Alzheimer’s disease or Frontotemporal dementia. Thus, a local analysis of the cortical complexity of regions more prone to change will likely increase the sensitivity and specificity of the analysis.

There are a number of important future analyses that can come from this study. Certainly obtaining longitudinal data on the subjects in the database (along with corresponding neuropsychological testing) will be important for understanding the trajectory of cortical complexity on an

individual basis. Given that the older subjects in this study grew up in a very different environment than the current younger subjects, the natural history may very well be changing and is a known limitation of cross-sectional designs. Following subjects who subsequently proceed to develop age-related neurodegenerative diseases such as Alzheimer's may also help to identify early cortical complexity changes that might indicate impending disease. Epidemiologic factors such as a history of hypertension, stroke, or diabetes, are also important factors to consider, but will require a different population than was used for this study. Finally, correlating complexity changes with other imaging biomarkers (such as the presence of cortical beta-amyloid protein deposition) may yield additional insight into cortical complexity changes across the lifespan, as will utilizing cortical complexity as a predictor of cognitive performance in normal aging and in dementia.

3.6 Conclusions

The results of this study demonstrate that complexity of the cerebral cortex linearly decreases during the course of even normal aging, quantified by computing the global fractal dimension of the cortical ribbon. As fractal dimension is a direct measure of gray matter atrophy and underlying cytoarchitectural changes, this is an important finding in regards to shape complexity of the cerebral cortex.

3.7 Acknowledgements

I thank Dr. Denise Park, the PI of the Center for Vital Logevity at University of Texas-Dallas, for providing access to the Dallas Lifespan Brain study database. Also, I would like to acknowledge contributions of Dr. Kristen Kennedy and Dr. Karen Rodrigue at the University of Texas-Dallas and Dr. Richard King, Brandon Brown, and Jeanette Berberich at the Alzheimer's Image Analysis Lab at the University of Utah.

This research was supported by the Center for Alzheimer's Care, Imaging and Research and grants from the National Institute of Aging (5R37AG006265-27, K23AG03835).

3.8 References

[1] K. Walhovd, L. Westlye, I. Amlien, T. Espeseth, I. Reinvang, N. Raz, I. Agartz, D. Salat, D. Greve, B. Fischl, A. Dale and A. Fjell, "Consistent neuroanatomical age-related volume differences across multiple samples," Neurobiology of Aging, vol. 32, no. 5, pp. 916-932, 2011.

[2] N. Raz, "Regional brain changes in aging healthy adults: general trends, individual differences and modifiers," Cerebral Cortex, vol. 15, no. 11, pp. 1676-1689, 2005.

[3] N. Raz, P. Ghisletta, K. Rodrigue, K. Kennedy and U. Lindenberger, "Trajectories of brain aging in middle-aged and older adults: regional and individual differences," NeuroImage, vol. 51, no. 2, pp. 501-511, 2010.

[4] A. Fotenos, A. Snyder, L. Girton, J. Morris and R. Buckner, "Normative estimates of cross-sectional and longitudinal brain volume decline in aging and AD," Neurology, vol. 64, no. 6, pp. 1032-1039, 2005.

[5] Y. Ge, R. I. Grossman, J. S. Babb, M. L. Rabin, L. J. Mannon, D. L. Kolson, "Age-related total gray matter and white matter changes in normal adult brain. Part II: quantitative magnetization transfer ratio histogram analysis," American Journal of Neuroradiology, vol. 23, no. 8, pp. 1334-1341, 2002.

[6] P. Thompson, K. M. Hayashi, G. De Zubicaray, A. L. Janke, S. E. Rose, J. Semple, A. W. Toga, "Dynamics of gray matter loss in Alzheimer"s disease," The Journal of Neuroscience, vol. 23, no. 3, pp. 994-1005, 2003.

[7] N. Raz, K. Rodrigue, K. Kennedy and J. Acker, "Vascular health and longitudinal changes in brain and cognition in middle-aged and older adults.," Neuropsychology, vol. 21, no. 2, pp. 149-157, 2007.

[8] E. Bullmore, M. Brammer, I. Harvey, R. Persaud, R. Murray and M. Ron, "Fractal analysis of the boundary between white matter and cerebral cortex in magnetic resonance images: a controlled study of schizophrenic and manic-depressive patients," Psychological Medicine, vol. 24, no. 03, p. 771, 1994.

[9] S. Free, S. Sisodiya, M. Cook, D. Fish and S. Shorvon, "Three-dimensional fractal analysis of the white matter surface from magnetic resonance images of the human brain," Cerebral Cortex, vol. 6, no. 6, pp. 830-836, 1996.

[10] M.A. Hofman, "The fractal geometry of convoluted brains," Journal fur Hirnforschung, vol 32, no. 1, pp. 103-111, 1990.

[11] K. Im, J. Lee, U. Yoon, Y. Shin, S. Hong, I. Kim, J. Kwon and S. Kim, "Fractal dimension in human cortical surface: multiple regression analysis with cortical thickness, sulcal depth, and folding area," Human Brain Mapping, vol. 27, no. 12, pp. 994-1003, 2006.

[12] J. Jiang, W. Zhu, F. Shi, Y. Zhang, L. Lin and T. Jiang, "A robust and accurate algorithm for estimating the complexity of the cortical surface," Journal of Neuroscience Methods, vol. 172, no. 1, pp. 122-130, 2008.

[13] V. Kiselev, K. Hahn and D. Auer, "Is the brain cortex a fractal?," NeuroImage, vol. 20, no. 3, pp. 1765-1774, 2003.

[14] J. Lee, U. Yoon, J. Kim, I. Kim, D. Lee, J. Kwon and S. Kim, "Analysis of the hemispheric asymmetry using fractal dimension of a

skeletonized cerebral surface," IEEE Transactions on Biomedical Engineering, vol. 51, no. 8, pp. 1494-1498, 2004.

[15] S. Majumdar, J. Lin, T. Link, J. Millard, P. Augat, X. Ouyang, D. Newitt, R. Gould, M. Kothari and H. Genant, "Fractal analysis of radiographs: assessment of trabecular bone structure and prediction of elastic modulus and strength," Med. Phys., vol. 26, no. 7, p. 1330, 1999.

[16] B. Mandelbrot, The fractal geometry of nature. New York: W.H. Freeman, 1983.

[17] D. Bresson and B. Mandelbrot, "Fractals: form, chance, and dimension," Leonardo, vol. 12, no. 3, pp. 248, 1979.

[18] P. Bourke, "Fractal landscapes," [online] 2003, http://astronomy.swin.edu.au/~pbourke/.

[19] F. Esteban, J. Sepulcre, N. de Mendizábal, J. Goñi, J. Navas, J. de Miras, B. Bejarano, J. Masdeu and P. Villoslada, "Fractal dimension and white matter changes in multiple sclerosis," NeuroImage, vol. 36, no. 3, pp. 543-549, 2007.

[20] J. Liu, L. Zhang and G. Yue, "Fractal dimension in human cerebellum measured by magnetic resonance imaging," Biophysical Journal, vol. 85, no. 6, pp. 4041-4046, 2003.

[21] L. Zhang, D. Dean, J. Liu, V. Sahgal, X. Wang and G. Yue, "Quantifying degeneration of white matter in normal aging using fractal dimension," Neurobiology of Aging, vol. 28, no. 10, pp. 1543-1555, 2007.

[22] L. Zhang, J. Liu, D. Dean, V. Sahgal and G. Yue, "A three-dimensional fractal analysis method for quantifying white matter structure in human brain," Journal of Neuroscience Methods, vol. 150, no. 2, pp. 242-253, 2006.

[23] Y. Wu, K. Shyu, C. Jao, Z. Wang, B. Soong, H. Wu and P. Wang, "Fractal dimension analysis for quantifying cerebellar morphological change of multiple system atrophy of the cerebellar type (MSA-C)," NeuroImage, vol. 49, no. 1, pp. 539-551, 2010.

[24] M. Cook, S. Free, M. Manford, D. Fish, S. Shorvon and J. Stevens, "Fractal description of cerebral cortical patterns in frontal lobe epilepsy," European Neurology, vol. 35, no. 6, pp. 327-335, 1995.

[25] T. Ha, U. Yoon, K. Lee, Y. Shin, J. Lee, I. Kim, K. Ha, S. Kim and J. Kwon, "Fractal dimension of cerebral cortical surface in schizophrenia and obsessive–compulsive disorder," Neuroscience Letters, vol. 384, no. 1-2, pp. 172-176, 2005.

[26] A. Sandu, I. Rasmussen, A. Lundervold, F. Kreuder, G. Neckelmann, K. Hugdahl and K. Specht, "Fractal dimension analysis of MR images reveals grey matter structure irregularities in schizophrenia," Computerized Medical Imaging and Graphics, vol. 32, no. 2, pp. 150-158, 2008.

[27] M. Casanova, D. Daniel, T. Goldberg, R. Suddath and D. Weinberger, "Shape analysis of the middle cranial fossa of schizophrenic patients: A computerized tomographic study," Schizophrenia Research, vol. 2, no. 1-2, p. 133, 1989.

[28] M. F. Casanova, "Quantitative shape analysis of the temporal and prefrontal lobes of schizophrenic patients: a magnetic resonance image study," JNP, vol. 2, no. 4, pp. 363-372, 1990.

[29] P. Thompson, "Abnormal cortical complexity and thickness profiles mapped in Williams Syndrome," Journal of Neuroscience, vol. 25, no. 16, pp. 4146-4158, 2005.

[30] Y. Wu, K. Shyu, T. Chen and W. Guo, "Using three-dimensional fractal dimension to analyze the complexity of fetal cortical surface from magnetic resonance images," Nonlinear Dynamics, vol. 58, no. 4, pp. 745-752, 2009.

[31] R. King, A. George, T. Jeon, L. Hynan, T. Youn, D. Kennedy and B. Dickerson, "Characterization of atrophic changes in the cerebral cortex using fractal dimensional analysis," Brain Imaging and Behavior, vol. 3, no. 2, pp. 154-166, 2009.

[32] R. King, B. Brown, M. Hwang, T. Jeon and A. George, "Fractal dimension analysis of the cortical ribbon in mild Alzheimer"s disease," NeuroImage, vol. 53, no. 2, pp. 471-479, 2010.

[33] R. Oldfield, "The assessment and analysis of handedness: the Edinburgh inventory," Neuropsychologia, vol. 9, no. 1, pp. 97-113, 1971.

[34] M. F. Folstein, S. E. Folstein, P. R. McHugh, "Mini-mental state: a practical method for grading the cognitive state of patients for the

clinician," Journal of psychiatric research, vol. 12, no. 3, pp. 189-198, 1975.

[35] B. Fischl, "FreeSurfer," Neuroimage, vol. 62, no. 2, pp. 774-781, 2012.

[36] A. Dale, B. Fischl and M. Sereno, "Cortical surface-based analysis," NeuroImage, vol. 9, no. 2, pp. 179-194, 1999.

[37] B. Fischl, A. Liu and A. Dale, "Automated manifold surgery: constructing geometrically accurate and topologically correct models of the human cerebral cortex," IEEE Transactions on Medical Imaging, vol. 20, no. 1, pp. 70-80, 2001.

[38] B. Fischl, D. Salat, E. Busa, M. Albert, M. Dieterich, C. Haselgrove, A. van der Kouwe, R. Killiany, D. Kennedy, S. Klaveness, A. Montillo, N. Makris, B. Rosen and A. Dale, "Whole brain segmentation," Neuron, vol. 33, no. 3, pp. 341-355, 2002.

[39] B. Fischl, M. Sereno and A. Dale, "Cortical surface-based analysis," NeuroImage, vol. 9, no. 2, pp. 195-207, 1999.

[40] B. Fischl, D. Salat, A. van der Kouwe, N. Makris, F. Ségonne, B. Quinn and A. Dale, "Sequence-independent segmentation of magnetic resonance images," NeuroImage, vol. 23, pp. S69-S84, 2004.

[41] X. Han, J. Jovicich, D. Salat, A. van der Kouwe, B. Quinn, S. Czanner, E. Busa, J. Pacheco, M. Albert, R. Killiany, P. Maguire, D. Rosas, N. Makris, A. Dale, B. Dickerson and B. Fischl, "Reliability of MRI-derived measurements of human cerebral cortical thickness: the effects of field strength, scanner upgrade and manufacturer," NeuroImage, vol. 32, no. 1, pp. 180-194, 2006.

[42] J. Jovicich, S. Czanner, D. Greve, E. Haley, A. van der Kouwe, R. Gollub, D. Kennedy, F. Schmitt, G. Brown, J. MacFall, B. Fischl and A. Dale, "Reliability in multi-site structural MRI studies: effects of gradient non-linearity correction on phantom and human data," NeuroImage, vol. 30, no. 2, pp. 436-443, 2006.

[43] F. Segonne, J. Pacheco and B. Fischl, "Geometrically accurate topology-correction of cortical surfaces using nonseparating loops," IEEE Transactions on Medical Imaging, vol. 26, no. 4, pp. 518-529, 2007.

[44] B. Fischl and A. Dale, "Measuring the thickness of the human cerebral cortex from magnetic resonance images," Proceedings of the National Academy of Sciences, vol. 97, no. 20, pp. 11050-11055, 2000.

[45] E. Kalmanti, T. G. Maris, "Fractal dimension as an index of brain cortical changes throughout life," in vivo, vol. 21, no. 4, pp. 641-646, 2007.

[46] G. Ziegler, R. Dahnke, L. Jäncke, R. Yotter, A. May and C. Gaser, "Brain structural trajectories over the adult lifespan," Human Brain Mapping, vol. 33, no. 10, pp. 2377-2389, 2011.

[47] A. Fjell, L. Westlye, H. Grydeland, I. Amlien, T. Espeseth, I. Reinvang, N. Raz, D. Holland, A. Dale and K. Walhovd, "Critical ages in the life course of the adult brain: nonlinear subcortical aging," Neurobiology of Aging, vol. 34, no. 10, pp. 2239-2247, 2013.

[48] L. Zhang, D. Dean, J. Liu, V. Sahgal, X. Wang and G. Yue, "Quantifying degeneration of white matter in normal aging using fractal dimension," Neurobiology of Aging, vol. 28, no. 10, pp. 1543-1555, 2007.

[49] L. Zhang, A. Butler, C. Sun, V. Sahgal, G. Wittenberg and G. Yue, "Fractal dimension assessment of brain white matter structural complexity post stroke in relation to upper-extremity motor function," Brain Research, vol. 1228, pp. 229-240, 2008.

[50] V. Rajagopalan, Z. Liu, D. Allexandre, L. Zhang, X. Wang, E. Pioro and G. Yue, "Brain white matter shape changes in Amyotrophic Lateral Sclerosis (ALS): a Fractal Dimension Study," PLoS ONE, vol. 8, no. 9, pp. e73614, 2013.

[51] F. Esteban, J. Sepulcre, J. de Miras, J. Navas, N. de Mendizábal, J. Goñi, J. Quesada, B. Bejarano and P. Villoslada, "Fractal dimension analysis of grey matter in multiple sclerosis," Journal of the Neurological Sciences, vol. 282, no. 1-2, pp. 67-71, 2009.

[52] J. Lin, N. Salamon, A. Lee, R. Dutton, J. Geaga, K. Hayashi, E. Luders, A. Toga, J. Engel and P. Thompson, "Reduced neocortical thickness and complexity mapped in mesial temporal lobe epilepsy with hippocampal sclerosis," Cerebral Cortex, vol. 17, no. 9, pp. 2007-2018, 2006.

[53] X. Li, J. Jiang, W. Zhu, C. Yu, M. Sui, Y. Wang and T. Jiang, "Asymmetry of prefrontal cortical convolution complexity in males with attention-deficit/hyperactivity disorder using fractal information dimension," Brain and Development, vol. 29, no. 10, pp. 649-655, 2007.

[54] A. Fjell, L. Westlye, I. Amlien, T. Espeseth, I. Reinvang, N. Raz, I. Agartz, D. Salat, D. Greve, B. Fischl, A. Dale and K. Walhovd, "High consistency of regional cortical thinning in aging across multiple samples," Cerebral Cortex, vol. 19, no. 9, pp. 2001-2012, 2009.

[55] A. Fjell, L. Westlye, H. Grydeland, I. Amlien, T. Espeseth, I. Reinvang, N. Raz, A. Dale and K. Walhovd, "Accelerating cortical thinning: unique to dementia or universal in aging?," Cerebral Cortex, vol. 24, no. 4, pp. 919-934, 2012.

[56] N. Raz, K. Rodrigue, D. Head, K. Kennedy and J. Acker, "Differential aging of the medial temporal lobe: a study of a five-year change," Neurology, vol. 62, no. 3, pp. 433-438, 2004.

[57] N. Raz, "Selective aging of the human cerebral cortex observed in vivo: differential vulnerability of the prefrontal gray matter," Cerebral Cortex, vol. 7, no. 3, pp. 268-282, 1997.

[58] E. Courchesne, H. Chisum, J. Townsend, A. Cowles, J. Covington, B. Egaas, M. Harwood, S. Hinds and G. Press, "Normal brain development and aging: quantitative analysis at in vivo MR imaging in healthy volunteers," Radiology, vol. 216, no. 3, pp. 672-682, 2000.

[59] K. Kennedy, K. Erickson, K. Rodrigue, M. Voss, S. Colcombe, A. Kramer, J. Acker and N. Raz, "Age-related differences in regional brain volumes: a comparison of optimized voxel-based morphometry to manual volumetry," Neurobiology of Aging, vol. 30, no. 10, pp. 1657-1676, 2009.

[60] E. Sowell, B. Peterson, P. Thompson, S. Welcome, A. Henkenius and A. Toga, "Mapping cortical change across the human life span," Nature Neuroscience, vol. 6, no. 3, pp. 309-315, 2003.

[61] N. Raz, F. Gunning-Dixon, D. Head, K. Rodrigue, A. Williamson and J. Acker, "Aging, sexual dimorphism, and hemispheric asymmetry of the cerebral cortex: replicability of regional differences in volume," Neurobiology of Aging, vol. 25, no. 3, pp. 377-396, 2004.

[62] J. Allen, J. Bruss, C. Brown and H. Damasio, "Normal neuroanatomical variation due to age: the major lobes and a parcellation of the temporal region," Neurobiology of Aging, vol. 26, no. 9, pp. 1245-1260, 2005.

[63] P. Curiati, J. Tamashiro, P. Squarzoni, F. Duran, L. Santos, M. Wajngarten, C. Leite, H. Vallada, P. Menezes, M. Scazufca, G. Busatto and T. Alves, "Brain structural variability due to aging and gender in cognitively healthy elders: results from the Sao Paulo Ageing and Health Study," American Journal of Neuroradiology, vol. 30, no. 10, pp. 1850-1856, 2009.

[64] D. Terribilli, M. Schaufelberger, F. Duran, M. Zanetti, P. Curiati, P. Menezes, M. Scazufca, E. Amaro, C. Leite and G. Busatto, "Age-related gray matter volume changes in the brain during non-elderly adulthood," Neurobiology of Aging, vol. 32, no. 2, pp. 354-368, 2011.

[65] N. Schuff, D. Tosun, P. Insel, G. Chiang, D. Truran, P. Aisen, C. Jack and M. Weiner, "Nonlinear time course of brain volume loss in cognitively normal and impaired elders," Neurobiology of Aging, vol. 33, no. 5, pp. 845-855, 2012.

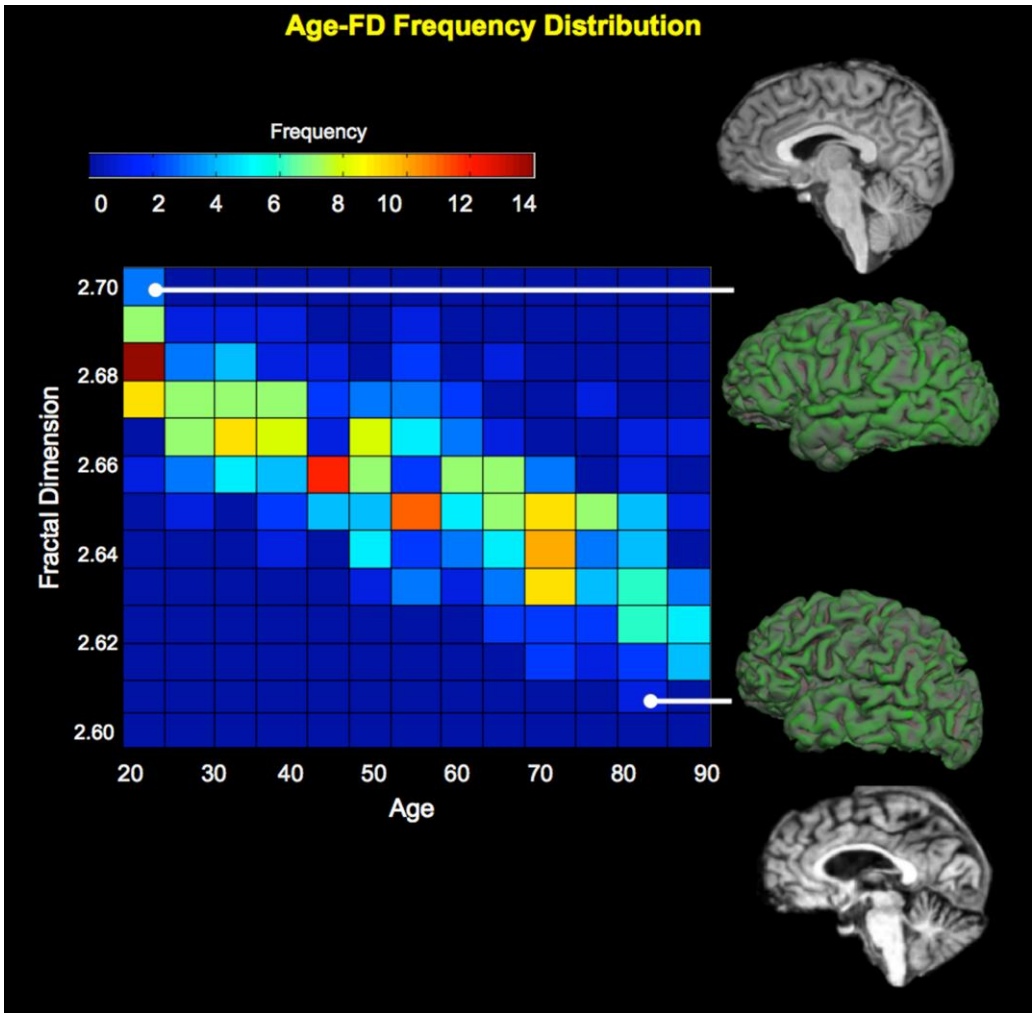

Figure 3.1 Color-coded frequency distribution plot (age vs. FD) of 301 cognitively normal subjects. The two sets of MR images and 3D surface models (via FreeSurfer) show the spectrum of cerebral cortical complexity in the dataset. One is of a 24-year-old person with a FD of 2.688 (top) and one is a 78-year-old person with a FD of 2.599 (bottom).

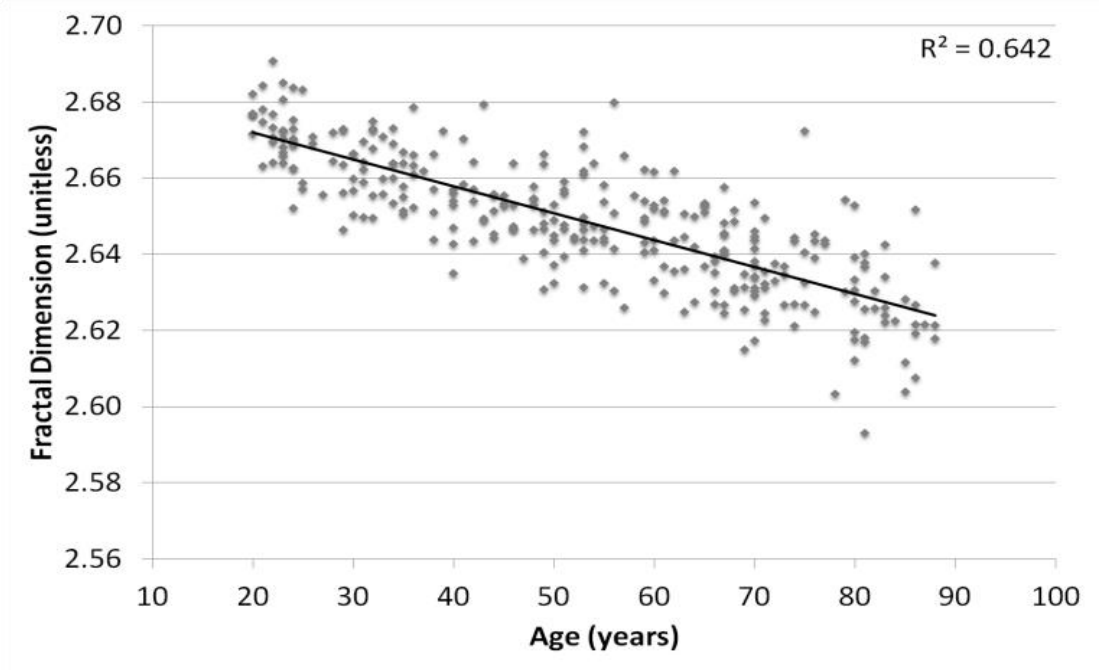

Figure 3.2 Fractal dimension across the lifespan. The scatter plot shows the age and cortical ribbon fractal dimension for each subject. The value of cortical fractal dimension tends to decrease as subjects age, but the variability in dimensionality for any give age rage increases as subjects age. The linear regression shows a high correlation.

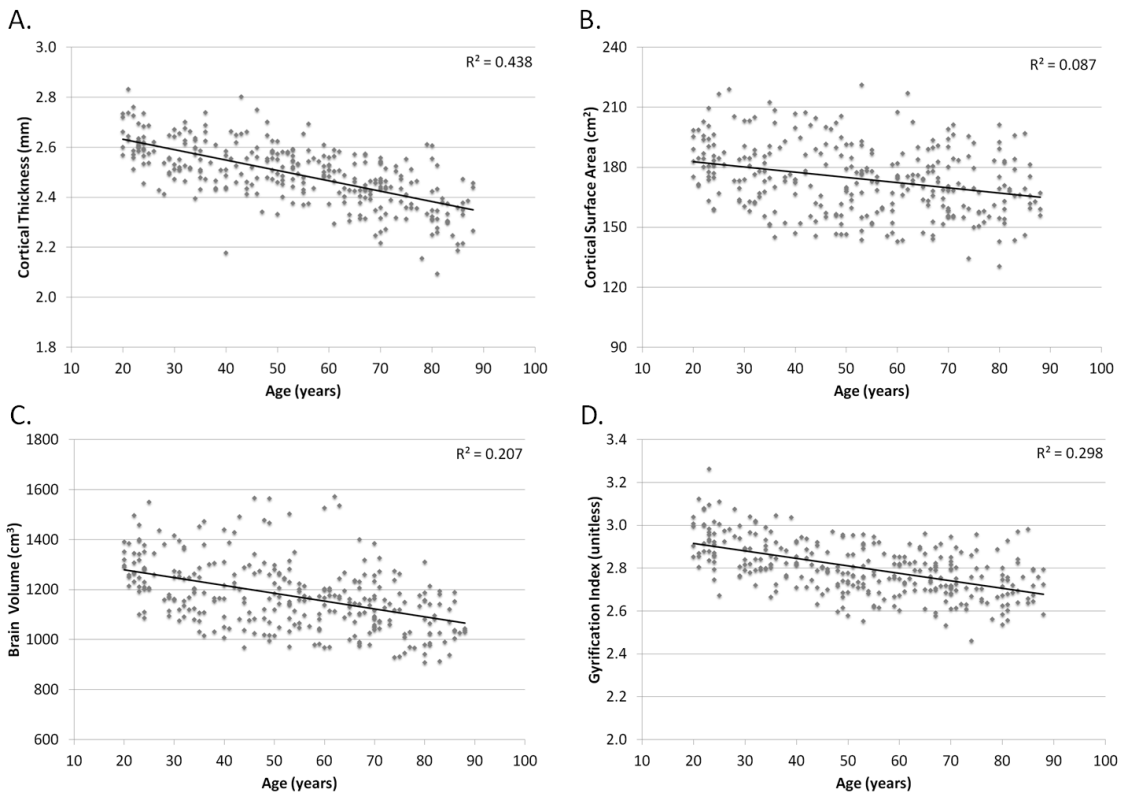

Figure 3.3 Selected volumetric properties as function of age. Each subject is represented as a point on the scatter plots. A. Cortical Thickness B. Cortical Surface Area. C. Brain Volume. D. Gyrification Index.

Table 3.1 Subject Demographics: All subjects are free from history of neurological disease or brain injury, claustrophobia, uncontrollable shaking, use of medications that affect cognitive function or vascular response, foreign metallic objects in the body, and any conditions which would contraindicate MRI. There is not a significant difference in the education, gender %, or MMSE score between any of the decade groups.

Age	Number	Gender (%M)	Education	MMSE
20-29	47	36.2%	16.4	29.0
30-39	42	38.1%	17.5	28.5
40-49	42	35.7%	16.0	28.5
50-59	47	30.4%	17.3	28.8
60-69	47	37.5%	16.9	28.2
70-79	41	34.1%	15.9	27.7
80-89	35	42.9%	15.9	27.1

Table 3.2 Summary statistics and differences per decade. The average values and standard deviations for each decade patients are shown in the table. The p values for the difference between the fractal dimensions of successive decade cohorts are shown in the right column. Significant differences ($p < 0.05$) are highlighted.

Decade	n	FD ± st. dev	*p* vs. previous decade	Sig. variance difference (F-test $p < 0.05$)
20s	47	2.670 ± 0.0090		vs. 80s
30s	42	2.662 ± 0.0092	*<0.0001*	vs. 70s, 80s
40s	42	2.652 ± 0.0091	*<0.0001*	vs. 80s
50s	46	2.649 ± 0.0113	0.0806	
60s	47	2.643 ± 0.0111	*0.0004*	
70s	41	2.636 ± 0.0119	*0.0178*	
80s	35	2.626 ± 0.0151	*0.0012*	

Table 3.3 General linear model: Cortical thickness and gyrification index were the factors with the highest predictive power of fractal dimension.

Model	Beta	Error	95% Lower bound	95% Upper bound
Cortical Thickness	0.088	0.004	0.080	0.096
Gyrification Index	0.071	0.004	0.062	0.079
Brain Volume	< 0.00001	0.000	-0.001	-0.120
Age	< 0.00001	0.000	0.000	-0.007
Surface Area	< 0.00001	0.000	-0.007	0.005

CHAPTER 4

USE OF AGE-WEIGHTED AND FRACTAL DIMENSION-WEIGHTED ATLASES TO CHARACTERIZE AGE-RELATED CEREBRAL CORTICAL ATROPHIC CHANGES ACROSS THE ADULT HUMAN LIFESPAN

4.1 Abstract

To assess cerebral cortical shape changes across the human lifespan by generating atlases, which are variably-weighted, geometrically averaged images of cerebral anatomy of a given population, age and global cerebral cortical fractal dimension (FD) were used as weighting variables. The purpose of this study was 1) to compare interatlas and intraatlas differences for age-weighted atlases and global cerebral cortical fractal dimension-weighted atlases and 2) to compare age-weighted atlases and global cerebral cortical fractal dimension-weighted atlases as biomarkers for cerebral cortical shape changes.

Magnetic resonance images of the brain from 314 subjects in the Dallas Lifespan Brain Study (age range 20-89, ~45 per decade) were

analyzed using FreeSurfer to segment volumetric parameters and generate 3D surface models of the cortex. The cortical fractal dimension was computed from the surface models using customized cube-counting software. The Large Deformation Diffeomorphic Metric Mapping framework was used to construct atlases and to assign metric distances on the space of anatomical images to quantify similarity/dissimilarity in the shape of the cerebral cortex.

Variability in cerebral cortical structure is highest in brains of higher age and lower fractal dimension. There is less variance in cerebral cortical structure for brains of equivalent fractal dimension as compared to brains of equivalent age. There is more variance in cerebral cortical structure between fractal dimension-weighted cohorts as compared to variance in cerebral cortical structure between age-weighted cohorts. Atlases weighted by fractal dimension capture more of the variance in cortical shape than atlases based upon age ($R^2_{FD} = 0.62$ & $R^2_{Age} = 0.48$).

Atlases weighted by fractal dimension is a novel concept that can capture cerebral cortical shape change better than age-weighted atlases.

4.2 Introduction

It is well established that during the normal aging process significant changes in the size and shape of the brain occur, which are not associated with cognitive dysfunction [1,2]. Additionally, there is a great amount of variability between different individuals within similar age groups in the

normal aging process. Different individuals "age" differently, i.e., at different rates of degeneration and at different regions within the brain [1,3]. These age-related changes, between different age groups and within similar age groups, in the shape of the brain with normal aging make age-appropriateness difficult to reliably assess and confound diagnoses in clinical practice. Therefore, quantification of these age-related changes and calibration for age using a large database of brains from cognitively normal subjects across the adult human lifespan will enable currently subjective measures of "age-appropriate" atrophy to be objectively quantified, and thus improve our understanding of age-related atrophic changes on an individual basis and across the lifespan. Also, we have created fractal dimension-weighted atlases and analyzed its use to capture cerebral cortical shape changes.

AtlasWerks was used to generate age-weighted and global fractal dimension-weighted atlases. The AtlasWerks suite is an open-source software package developed by the Scientific Computing and Imaging Institute at the University of Utah, as an implementation of the deformation algorithms based on the well-established Large Deformation Diffeomorphic Metric Mapping (LDDMM) framework. The Large Deformation Diffeomorphic Metric Mapping framework has been used to estimate geodesics in the diffeomorphic space, where the optimal diffeomorphisms are the shortest metric distances between images [4-9]. Also, the LDDMM framework has

been used to measure interpopulation [10,11] and intrapopulation [12] variability. Please see [8,13] to review use of diffeomorphic mappings for modeling anatomical shape changes.

AtlasWerks simultaneously and reversibly deforms a set of images into a geometric average, an atlas. The influence of each image on the atlas has been weighted by age and fractal dimension, using a sliding Gaussian Kernel, to generate age-weighted and global fractal dimension-weighted atlas. Here, we used AtlasWerks to construct age-weighted atlases for every half-decade from age 20 to 89 and fractal dimension-weighted atlases in increments of FD= 0.01 from FD of 2.60 to 2.69, using a database of 314 cognitively normal brains collected by the Dallas Lifespan Brain Study. Each cortical voxel of an atlas has a unique set of statistical values based upon location and age and fractal dimension. Also, we used the concept of "vector energy" within the LDDMM framework to assign metric distances on the space of anatomical images to quantify interatlas differences and intraatlas variability in the shape of the cerebral cortex.

To the best of our knowledge, this is the first large, cross-sectional study to 1) apply age-weighted atlases to quantitatively characterize age-related atrophic changes through the adult human lifespan (age: 20-89) for a cognitively normal cohort, 2) apply fractal dimension-weighted atlases to quantitatively characterize atrophic changes for a cognitively normal cohort, 3) apply vector energy to quantify the variability in the shape of the cerebral

cortex within atlases of age and global fractal dimension (intraatlas analysis), and 4) apply vector energy to quantify the difference in shape of the cerebral cortex between successive atlases of age and global fractal dimension (interatlas analysis).

4.3 Methodology

The methodology that has been used in this paper to construct age-weighted and global cerebral cortical complexity-weighted atlases has been outlined in Figure 4.1. All preprocessing steps have used Mac OS X version 10.5.8.

4.3.1 Participants

For this study, 314 subjects from DLBS were analyzed. Subjects have at least a high school education, a Mini-Mental State Exam (MMSE) of 26 or greater, and corrected vision of 20/30. Subjects are free from history of neurological disease or brain injury, claustrophobia, uncontrollable shaking, use of medications that affect cognitive function or vascular response, foreign metallic objects in the body, and any conditions which would contraindicate MRI. For more information on DLBS see Chapter 3 Sections 3.3.1 and 3.3.2.

4.3.2 Image Analysis Pipeline

Image analysis steps are the same as outlined in Section 3.3.3 in Chapter 3.

4.3.3 Atlas Construction Using LDDMM Framework

4.3.3.1 Intensity Normalization

All 314 images have been intensity normalized via a semiautomated process. Each image has been normalized based on binning of the intensity ranges of gray matter, white matter, and cerebrospinal fluid. Subsequently, the intensity histograms have been manually corrected for these different tissue classes in the brain. This second intensity normalization is performed to standardize intensity for this particular cohort of 314 images.

4.3.3.2 Affine Alignment to Common Coordinate Space

Prior to atlas construction, in order to remove artifacts due to scanner positions and pose, all the images were aligned to one image in the population.

4.3.3.3 Gaussian Binning

To construct age-weighted and FD-weighted atlases, the subjects were binned using a Gaussian kernel to create age-weighted and FD-weighted cohorts. Age-weighted cohorts were created for every half-decade from ages

20-89 using a Gaussian kernel to bin with sigma=5. Fractal dimension-weighted cohorts were created from fractal dimension 2.60-2.69 using a Gaussian kernel to bin with sigma=0.01. The following is the kernel that was used:

$$w(t_i,t) = \frac{1}{\sqrt{2\pi\sigma}} \exp \frac{-(t_i,t)^2}{2\sigma^2} \tag{4.1}$$

4.3.3.4 Age-weighted and Fractal Dimension-Weighted Atlas Construction Using LDDMM Framework

Atlases were constructed using AtlasWerks, which is based on the well-established Large Deformation Diffeomorphic Metric Mapping framework. Under the LDDMM framework, brain shape changes are modeled by diffeomorphisms acting on the underlying coordinate space of images [10]. Diffeomorphisms are one-to-one, smooth, and invertible transformations that preserve topology and form a group structure under compositions. Any two images can be represented by a diffeomorphism that registers them. This group of diffeomorphisms is a manifold with a Riemannian metric. This metric defines the notion of similarity and alternatively, the difference between brain shapes.

A convenient and natural machinery for generating diffeomorphic transformations is by the integration of ordinary differential equations (ODE) on the underlying coordinate space, Ω defined via the smooth time-indexed

velocity vector fields $v(t, y) : (t \in [0, 1], y \in \Omega) \rightarrow R3$. The function $\varphi v(t, x)$ given by the solution of the ODE $dy/dx = v(t, y)$ with the initial condition $y(0) = x$ defines a diffeomorphism of Ω. One defines a Riemannian metric on a space of diffeomorphisms by inducing an energy on these velocity fields.

The distance between the identity transformation and a diffeomorphism ψ is defined as the minimization

$$d(id, \psi)^2 = \min\{\int_0^1 \langle Lv(t,\cdot), v(t,\cdot)\rangle dt : \phi^v(1,\cdot) = \psi(\cdot)\} \tag{4.2}$$

The distance between any two diffeomorphisms is defined as $d(\varphi, \psi) = d(id, \psi \circ \varphi^{-1})$. This Riemannian metric defined on the space of diffeomorphisms can now be used to compute a deformation that matches two images. If the problem is to register an image I^1 over the target image I^2, then image at time t is defined as $I^t = I^1 \circ \varphi^{-1}$, i.e., $I^0 = I^1$. The deformation φ is defined as the 'optimal' time-varying velocity field $\hat{v}$, based on minimizing the energy functional, $E(v)$:

$$\mathrm{E}(v) = \int_0^1 \langle Lv(t,\cdot), v(t,\cdot)\rangle^2 dt + \frac{1}{\sigma^2}\left\| I^1 \circ \phi^{-1} - I^2 \right\|_{L^2}^2, \tag{4.3}$$

i.e.,

$$\begin{aligned} &\hat{v} = \arg\min \mathrm{E}(v), \\ &v : \dot{\phi}_t = v_t(\phi_t) \end{aligned} \tag{4.4}$$

where the second term in Equation 3 allows inexact matching, and σ is a free parameter controlling the tradeoff between exactness of the match and smoothness of the velocity fields.

Notice that the above metric induces a distance metric between two images, I^1 and I^2 written as a minimizer of the form:

$$d(I^1, I^2)^2 = \min\{Vector \text{ energy} + \text{Image energy}\} \tag{4.5}$$

The metric defines the notion of similarity and alternatively, the difference between brain shapes. Notice, the first term, vector energy, can be also be interpreted as the minimum amount of energy it takes to deform one brain in a smooth and invertible fashion to match another and the second term, image mismatch, allows for inexact matching of images.

The empirical estimate of weighted Fréchet mean of images, $\bar{I}$ can now be presented using this distance metric on images. The goal is to compute the unbiased weighted atlas image, $\bar{I}$ that minimizes the sum of squared distances to the given population of images [10].

Given a collection of N anatomical images and corresponding normalized weights, $\{I^i, w^i\}$ for $i = 1, \cdots, N$, the atlas can be defined as a solution to the minimum mean square energy criteria

$$\bar{I} = \arg\min_I \frac{1}{N} \sum_{i=1}^{N} w^i d(I, I^i)^2 \tag{4.6}$$

The minimum mean squared energy atlas construction problem is that of jointly estimating an image $\bar{I}$ and N individual deformations.

We use the above framework to create age-weighted $\bar{I}^l_{age}$ and FD-weighted $\bar{I}^m_{age}$ atlas where l and m indexes over the chosen age and FD grid points. Furthermore, we have calculated the amount of vector energy it takes

to deform an individual constituent image to the respective atlas for all age-weighted and FD-weighted atlases. This is used to calculate intraatlas variability in shape of the images for both sets of atlases.

The values of vector energies required to deform an individual image to the respective atlas between successive half-decade-wide cohorts have been compared using a Student's t-test (2 tailed, model 3, $p < 0.05$ considered significant).

4.4 Results

4.4.1 Results for Age-Weighted Atlases Analyses

4.4.1.1 Age-Weighted Atlases Quantitatively Characterize Age-Related Atrophic Changes Through the Adult Human Lifespan

Age-weighted atlases have been constructed for every half-decade from ages 20-89 using a Gaussian kernel to bin with sigma=5. Each age-weighted atlas is a statistical representation of that population, i.e., age-weighted atlas 20 (binned with a Gaussian kernel of mean=20 and sigma=5) represents the shapes of all the cerebral cortices of individuals that are of age ≤25. Figure 4.2 illustrates the changes in the shape of the cerebral cortex with normal aging for every two decades from 20 to 80.

The amount of vector energy it takes to deform each image to its respective atlas has been calculated and plotted for all age-weighted atlases in the DLBS database (Figure 4.3). Each datum represents the images of each atlas, keeping in mind a Gaussian kernel was used for binning. The amount of vector energy it takes to deform each image to its respective atlas increases with age and there is more variability in the shape of the cerebral cortex in younger individuals and older individuals.

4.4.1.2 Intraatlas Analysis for Age-Weighted Atlases

The amount of vector energy it takes to construct each atlas quantifies the variability in the shape of the cerebral cortex within each decade and half-decade. We found that the amount of vector energy it takes to construct each atlas remains approximately constant until age 55 and then increases with age (see Figure 4.4). The increase vector energy necessary to construct each atlas after age 55 indicates greater variability in the shape of the cerebral cortex within the age groups (half-decade and decade after age 55).

A Student's t-test (2 tailed, model 3) to compare the amount of vector energy to deform each image to its respective atlas for successive half-decade atlases has been performed. We found that there is no significant difference in the amount of vector energy it takes to deform an image to its respective atlas for successive atlases from 20-55. Significant differences ($p<0.05$) in vector energy to deform each image to its respective atlas for successive half-

decade atlases have been highlighted in yellow. There was significant difference in the amount of vector energy it takes to deform each image to its respective atlas from 55-60, 60-65, 65-70, & 75-80 (Table 4.1).

Here, a Student's t-test (2 tailed, model 3) to compare the amount of vector energy to deform each image to its respective atlas for successive decade atlases has been performed. We found similar results as the aforementioned half-decade analysis, with significant difference in the amount of vector energy it takes to deform each image to its respective atlas from 50-60, 60-70, & 70-80 (Table 4.2).

A Student's t-test (2 tailed, model 3) to compare the amount of vector energy to deform each image to its respective atlas for successive two-decade atlases has been performed. We found significant difference in the amount of vector energy it takes to deform each image to its respective atlas from 30-50, 40-60, 50-70, & 60-80 (Table 4.3).

The intraatlas analyses indicate that the amount of vector energy it takes to construct each atlas remains approximately constant until age 55 and then increases with age.

4.4.1.3 Interatlas Analysis for Age-Weighted Atlases

Vector energy quantifies the difference in the shape of the cerebral cortex between each decade and half-decade. Here, we have plotted the

amount of vector energy it takes to deform each atlas to the successive decade atlas (Figure 4.5). In this interatlas analysis, we found that the amount of vector energy it takes to deform each atlas to the successive decade-atlas increases with age, i.e., the difference in the shape of the cerebral cortex between decades increases with age. Also, we found similar results with lower sampling, i.e., with deforming each atlas to the successive half-decade atlas (data not shown).

Here, we use age-weighted Atlas 20 as a gold standard of cognitively normal and compare the vector energy required for each image in Atlas 20 to be deformed to the Atlas 20 image as compared to the vector energy required for each image to be deformed to its respective atlas. We found that there is a significant difference in the shape of the cerebral cortex between the atlases from age 55 onwards for the analysis with half-decades and from age 60 onwards for the analysis with decades (Table 4.4).

4.4.2 Results for Fractal Dimension-Weighted Atlases Analyses

4.4.2.1 Fractal Dimension-Weighted Atlases Quantitatively Characterize Age-Related Atrophic Changes

Fractal dimension-weighted cohorts were constructed from fractal dimension 2.60-2.69 using a Gaussian kernel to bin with sigma=0.01. Figure

4.6 illustrates the changes in the shape of the cerebral cortex with increase in global fractal dimension for every 0.03 FD from FD of 2.60 to 2.69.

The amount of vector energy it takes to deform an individual constituent image to its respective atlas has been calculated and plotted for all FD-weighted atlases in the DLBS database (Figure 4.7). We found that the amount of vector energy it takes to deform each image to its respective atlas decreases with increase in global cerebral cortical FD and there is more variability in the shape of the cerebral cortex in individuals with lower global cerebral cortical FD.

In comparison to age-weighted atlases, we see that atlases weighted by global fractal dimension capture more of the variance in cortical shape than atlases weighted by age, R^2=0.48 & R^2= 0.62, respectively.

4.4.2.2 Intraatlas Analysis for FD-Weighted Atlases

Vector energy quantifies the variability in the shape of the cerebral cortex within each decade and half-decade. We found that the amount of vector energy it takes to construct each atlas decreases with an increase in cortical FD (see Figure 4.8). The decrease vector energy necessary to construct each atlas indicates lesser variability in the shape of the cerebral cortex within the age groups (half-decade and decade).

4.4.2.3 Interatlas Analysis for FD-Weighted Atlases

Vector energy quantifies the difference in the shape of the cerebral cortex between each decade and half-decade. Here, we have plotted the amount of vector energy it takes to deform each global fractal dimension-weighted atlas to the successive atlas. In our interatlas analysis, we found that the amount of vector energy it takes to deform each atlas to the successive decade-atlas decreases with an increase in global cerebral cortical FD, i.e., the difference in the shape of the cerebral cortex between decades decreases with an increase in FD (Figure 4.9).

Also, we found that there is significant difference in the amount of vector energy it takes to deform each image to its respective atlas from 2.61-2.62, 2.62-2.63, 2.63-2.64, 2.64-2.65, 2.65-2.66, 2.66-2.67, & 2.68-2.69. Therefore, there is a significant difference in the shape of the cerebral cortex between the aforementioned FD-weighted atlases.

4.5 Discussion

In Chapter 3, we had used fractal dimension to quantify the shape of the cerebral cortex and the change in the fractal dimension metric to characterize the change in the shape of the cerebral cortex across the adult human lifespan. In this chapter, we have used vector energy to quantify and characterize the change in the shape of the cerebral cortex. We have

confirmed our previous finding of variability of the shape of the cerebral cortex increasing with normal aging. However, in this study with vector energy, we did not find a significant difference in the shape of the cerebral cortex between cohorts earlier than age 55, whereas we had reported significant difference in the shape of the cerebral cortex between 20s and 30s cohorts and between the 30s and 40s cohorts in Chapter 3, using fractal dimension. Furthermore, we found an acceleration of the difference in the shape of the cerebral cortex between atlases of higher age cohorts. Although, the assessment of trajectory of different measures with aging across the human lifespan is mixed in extant literature, our nonlinear trajectory assessment is in accord with findings by other groups [1,11,14]. Obtaining longitudinal data on the subjects in the database, along with corresponding neuropsychological testing, may help to understand the sources of the variability within and acceleration between age groups and the long-term clinical significance thereof.

In the process of deforming a population of images into a weighted atlas, some individual outliers were identified that required significantly more energy to deform from the native space into the atlas space. It is important to note that these outliers were the same individuals in the age-weighted and fractal-dimension weighted atlases (see Figures 4.3 and 4.7). Upon closer visual inspection, these individuals do appear to be structurally different from the rest of the population. For example, in creating the

weighted atlas centered around 75 years old, one individual had required much more vector energy (~800) to be deformed to the 75-year-old Atlas than the rest of the population (average energy ~250). When compared to the 75-year-old Atlas, this individual showed wider sulci, larger ventricles, and a thinner cortical ribbon diffusely. Note that despite the evidence for greater cerebral atrophy, the cognitive performance on screening tests was still within the normal range. The visual confirmation of structural differences helps to substantiate the notion that vector energy under the LDDMM framework is capturing the intended structural variability.

A useful extension of the approach used in the chapter is to create other biomarker-weighted atlases. Other than the structural changes due to normal aging and neurodegenerative disease, there are biochemical, metabolical, and pathological changes that occur as well. Atlases may be constructed by being weighted these other clinically relevant biomarkers. This may be more reliable as an indicator of intrapopulation variability and interpopulation differences and to augment clinical diagnosis.

Moreover, there are a number of important future analyses that can come from this study. Age-weighted atlases across the human lifespan can be used as a baseline to quantitatively characterize the normal aging process. Also, age-weighted atlases can be used to quantify and characterize changes due to different neurodegenerative diseases. Currently, the variability in structure due to normal aging, which is present concomitantly with the

structural changes due to neurodegenerative disease, confounds the diagnosis of neurodegenerative diseases. Having age-weighted atlases for normal aging and for neurodegenerative disease, we can then quantitatively delineate normal aging changes from changes due to a specific neurodegenerative disease and create quantitative characteristic plots for each neurodegenerative disease, without the confounding effects of normal aging.

4.6 Conclusions

Age-weighted atlases can quantitatively characterize age-related atrophic changes in the cerebral cortex and provide a baseline for and improve our understanding of cortical shape change with normal aging across the adult human lifespan. By accounting for the variability in the shape of the cortex between different individuals within specific age groups and quantifying differences between age groups, age-appropriateness on an individual basis becomes easier to assess.

Fractal dimension is a novel neuromaging biomarker that summarizes and quantifies clinically relevant changes in brain shape, which are a reflection of underlying physiological changes, which occur due to normal aging or neurodegenerative disease. Also, fractal dimension-weighted atlases capture the variance in cerebral cortical shape and shape change progression better than age-weighted atlases. Therefore, fractal dimension may be a better surrogate biomarker for cerebral cortical shape changes than age and

a better predictor of cerebral cortical shape change.

As a quantitative and reliable measure that can characterize shape changes in the cerebral cortex that accrue with normal aging and neurodegenerative diseases, global fractal dimension can provide a quantitative interpretation of structural data in neuroradiological scans that is complementary or not available by standard volumetric analyses. Consequently, using this quantitative metric, we may dissociate structural changes associated with aging from those caused by dementing neurodegenerative diseases. Furthermore, cerebral cortical FD, as a measure of structural changes, in addition to other quantitative markers, such as volumetric, metabolic, and pathological measures, may augment/replace the current standard of care of qualitative and subjective clinical diagnosis and may significantly improve clinical diagnosis of neurodegenerative disorders.

4.7 Acknowledgements

I thank Dr. Sarang Joshi for developing Atlaswerks and the seminal work supporting it. I thank Dr. Nikhil Singh's guidance in helping to learn how to use Atlaswerks. This study would not have been realized without the constructive discussions with and contributions from Carena Kole, Dr. P. Thomas Fletcher and Dr. Richard King. Finally, I thank Kyle Hansen, Jeanette Berberich, and Brandon Brown for their assistance.

This study was supported by the Center for Alzheimer's Care Imaging and Research at the University of Utah, and grants from the Robert Wood Johnson Foundation, National Institute of Aging (5-R37-AG006265-27 and 5-P30-AG012300-15), and the Alzheimer's Association.

4.8 References

[1] N. Raz, "Regional brain changes in aging healthy adults: general trends, individual differences and modifiers," Cerebral Cortex, vol. 15, no. 11, pp. 1676-1689, 2005.

[2] K. Walhovd, L. Westlye, I. Amlien, T. Espeseth, I. Reinvang, N. Raz, I. Agartz, D. Salat, D. Greve, B. Fischl, A. Dale and A. Fjell, "Consistent neuroanatomical age-related volume differences across multiple samples," Neurobiology of Aging, vol. 32, no. 5, pp. 916-932, 2011.

[3] N. Raz, P. Ghisletta, K. Rodrigue, K. Kennedy and U. Lindenberger, "Trajectories of brain aging in middle-aged and older adults: regional and individual differences," NeuroImage, vol. 51, no. 2, pp. 501-511, 2010.

[4] M. I. Miller, L. Younes, "Group actions, homeomorphisms, and matching: a general framework," International Journal of Computer Vision, vol. 41, no. 1-2, pp. 61-84, 2001.

[5] A. Trouvé and L. Younes, "Metamorphoses through lie group action," Found Comput Math, vol. 5, no. 2, pp. 173-198, 2005.

[6] M. Beg, M. Miller, A. Trouvé and L. Younes, "Computing large deformation metric mappings via geodesic flows of diffeomorphisms," International Journal of Computer Vision, vol. 61, no. 2, pp. 139-157, 2005.

[7] L. Younes, A. Qiu, R. Winslow and M. Miller, "Transport of relational structures in groups of diffeomorphisms," Journal of Mathematical Imaging and Vision, vol. 32, no. 1, pp. 41-56, 2008.

[8] L. Younes, F. Arrate and M. Miller, "Evolutions equations in computational anatomy," NeuroImage, vol. 45, no. 1, pp. S40-S50,

2009.

[9] M. Miller, A. Trouvé and L. Younes, "On the metrics and Euler-Lagrange equations of computational anatomy," Annual Review of Biomedical Engineering, vol. 4, no. 1, pp. 375-405, 2002.

[10] S. Joshi, B. Davis, M. Jomier and G. Gerig, "Unbiased diffeomorphic atlas construction for computational anatomy," NeuroImage, vol. 23, pp. S151-S160, 2004.

[11] J. Allen, J. Bruss, C. Brown and H. Damasio, "Normal neuroanatomical variation due to age: the major lobes and a parcellation of the temporal region," Neurobiology of Aging, vol. 26, no. 9, pp. 1245-1260, 2005.

[12] M. Miller, A. Trouvé and L. Younes, "Geodesic shooting for computational anatomy," Journal of Mathematical Imaging and Vision, vol. 24, no. 2, pp. 209-228, 2006.

[13] L. Younes, "Shapes and diffeomorphisms," Applied Mathematical Sciences, vol. 171, 2010.

[14] A. Fjell, L. Westlye, H. Grydeland, I. Amlien, T. Espeseth, I. Reinvang, N. Raz, A. Dale and K. Walhovd, "Accelerating cortical thinning: unique to dementia or universal in aging?," Cerebral Cortex, vol. 24, no. 4, pp. 919-934, 2012.

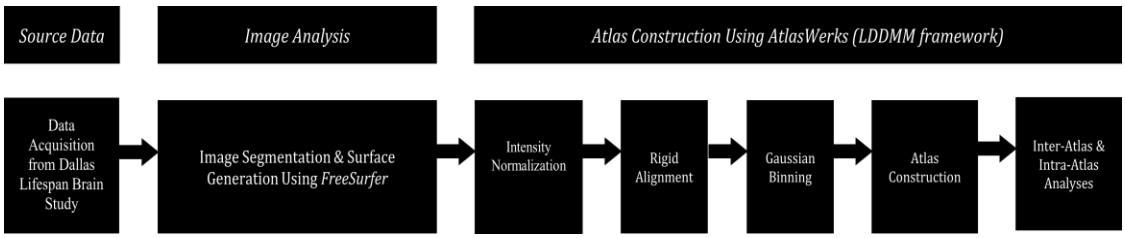

Figure 4.1 Pipeline showing overall methodology to construct age-weighted and cortical complexity weighted atlases.

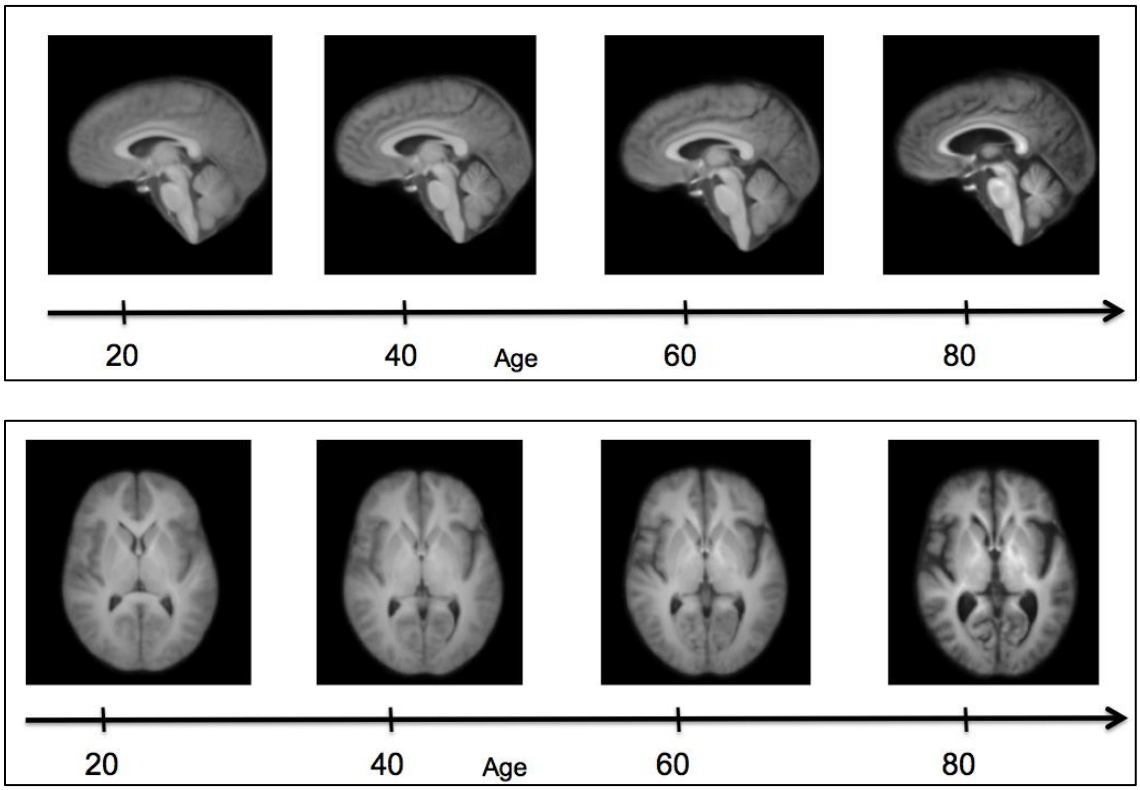

Figure 4.2 Sagittal (top panel) and axial (bottom panel) slices of age-weighted atlases for every two decades from 20 to 80 illustrate the changes in the shape of the cerebral cortex with normal aging.

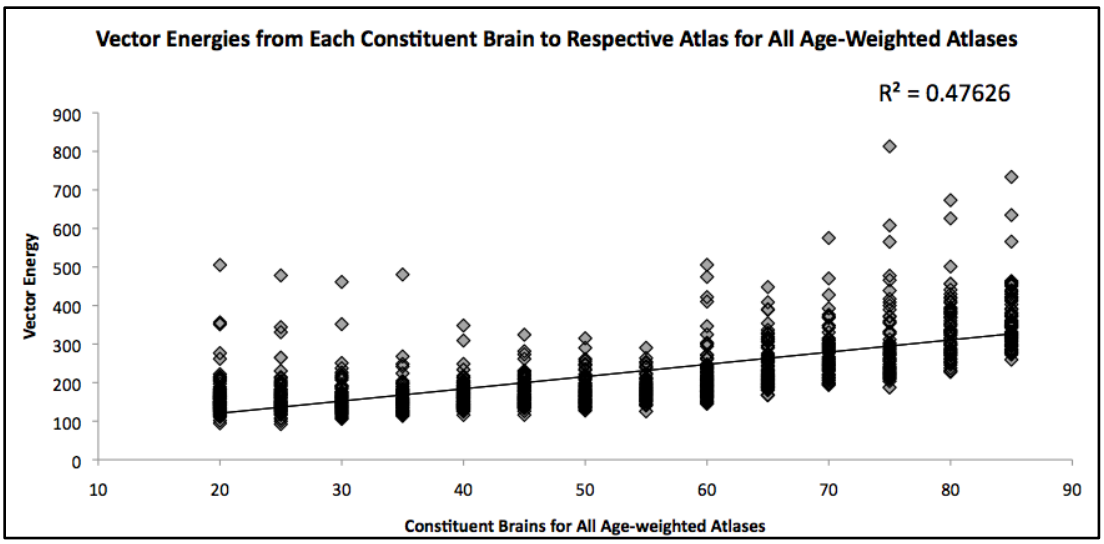

Figure 4.3 Amount of vector energy it takes to deform an individual constituent image to the respective atlas has been plotted for all age-weighted atlases in the DLBS database.

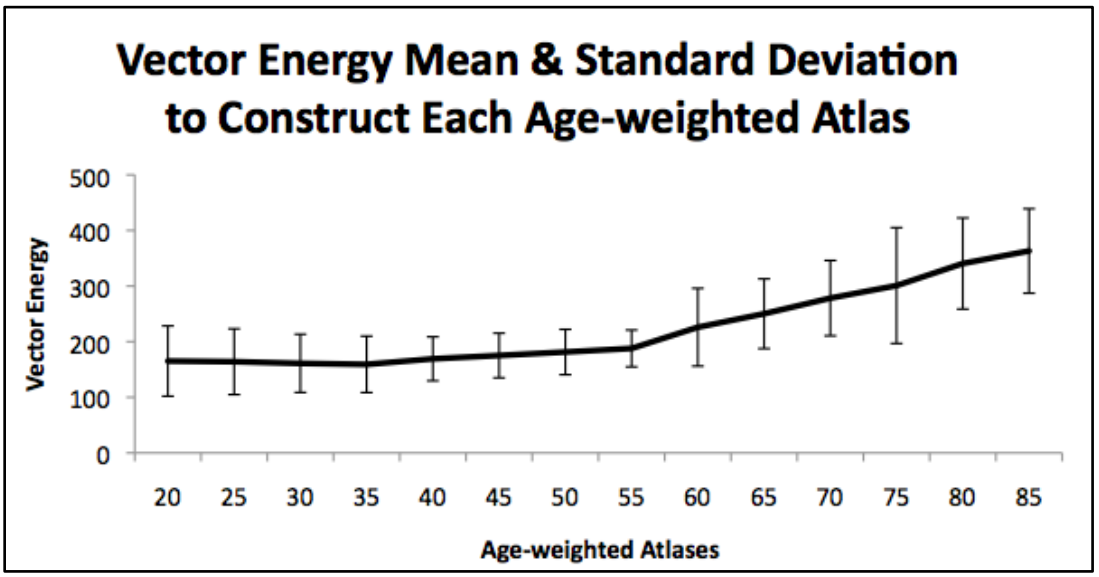

Figure 4.4 Intraatlas analysis of age-weighted atlases. Amount of vector energy it takes to deform each atlas to the successive decade-atlas increases with age, i.e., the difference in the shape of the cerebral cortex between decades increases with age.

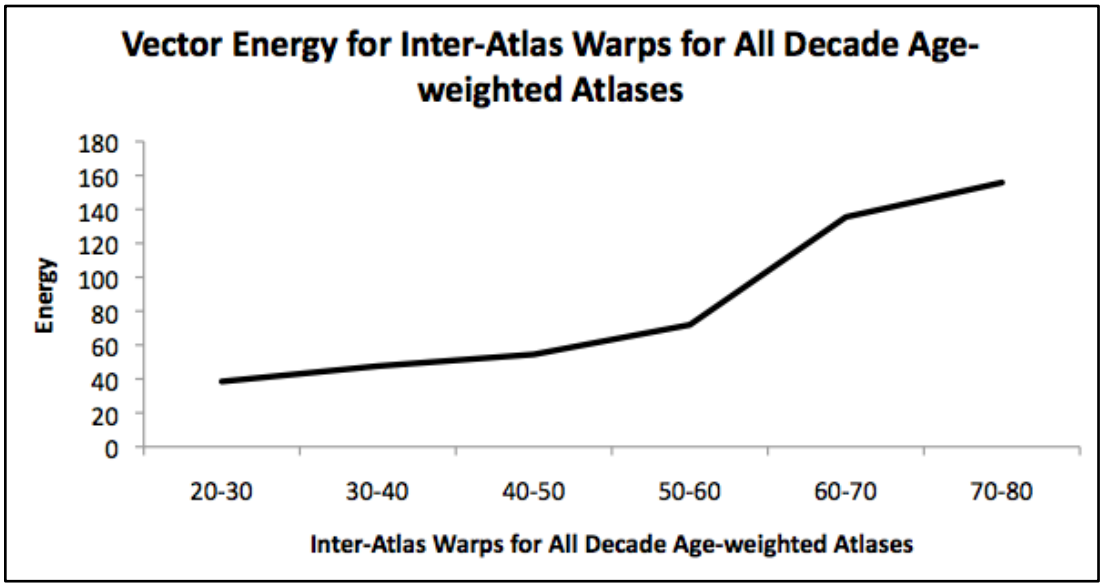

Figure 4.5 Interatlas analysis of age-weighted atlases. The amount of vector energy it takes to deform each atlas to the successive decade atlas increases linearly but with greater slopes between certain age groups.

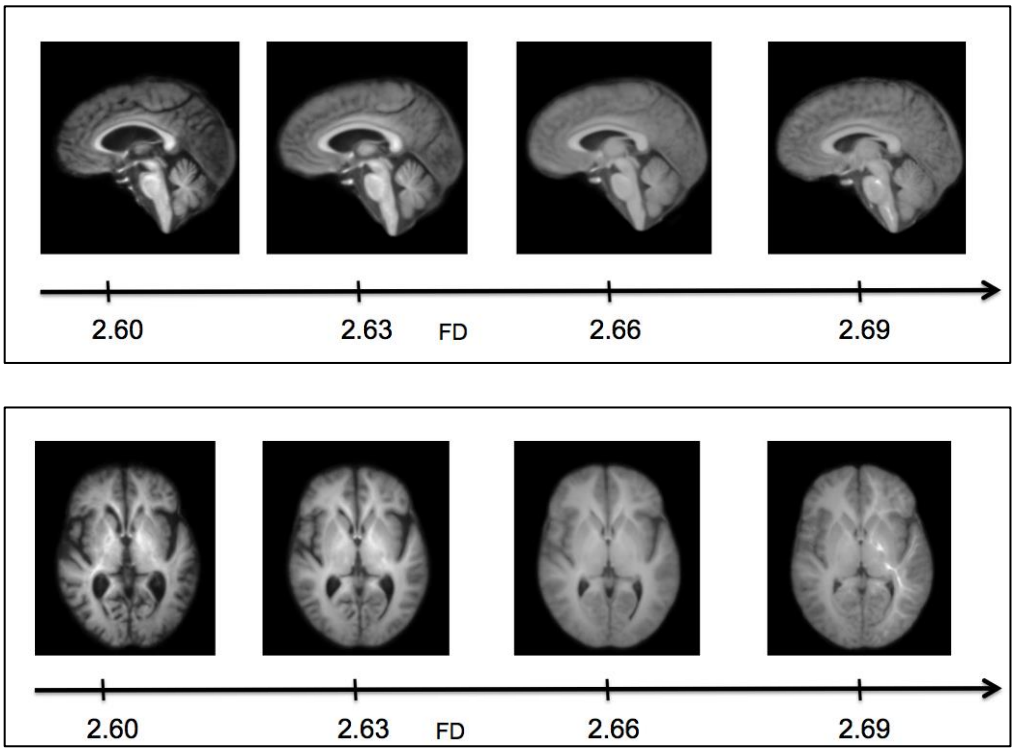

Figure 4.6 Sagittal (top panel) and axial (bottom panel) slices of fractal dimension-weighted atlases for every 0.03 FD from FD of 2.60 to 2.69 illustrate the changes in the shape of the cerebral cortex with increase in global FD.

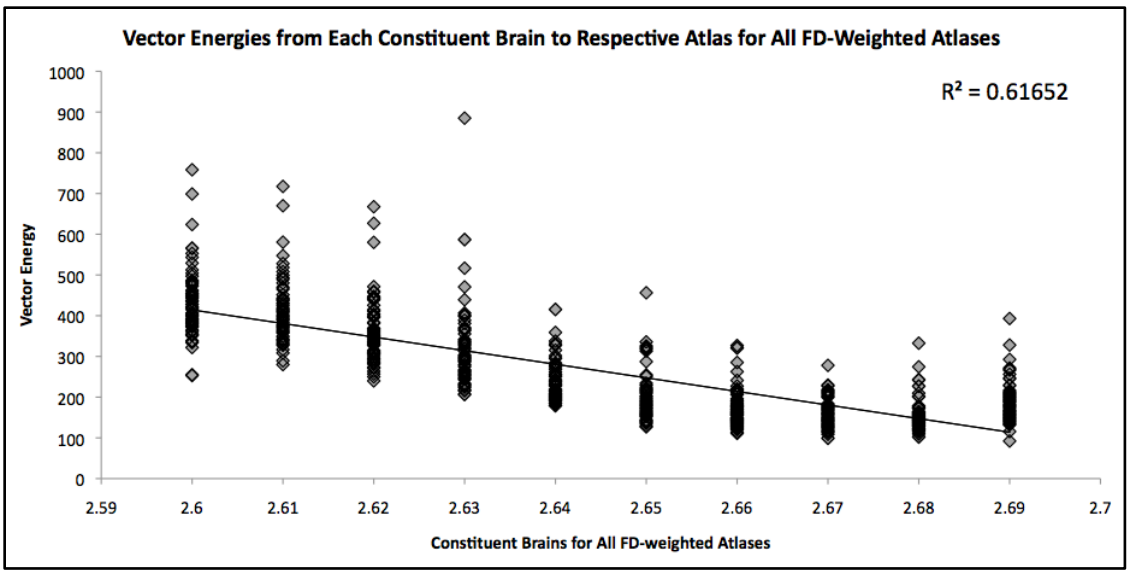

Figure 4.7 Amount of vector energy it takes to deform an individual constituent image to its respective atlas has been plotted for all global fractal dimension-weighted atlases in the DLBS database.

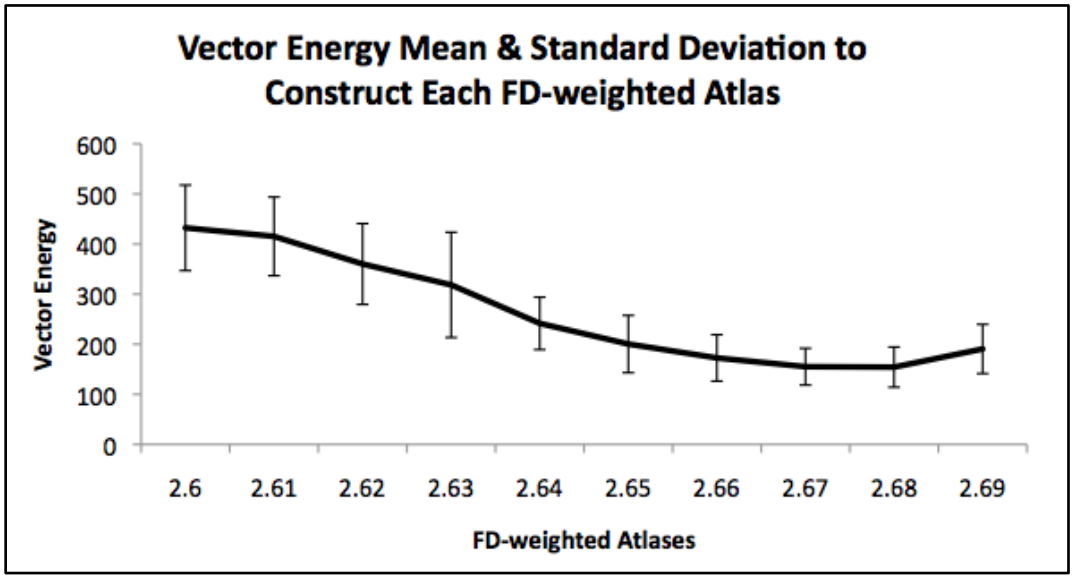

Figure 4.8 Intraatlas analysis of FD-weighted atlases. Amount of vector energy it takes to deform each atlas to the successive decade atlas decreases with an increase in global cerebral cortical FD, i.e., the difference in the shape of the cerebral cortex between decades decreases with an increase in FD.

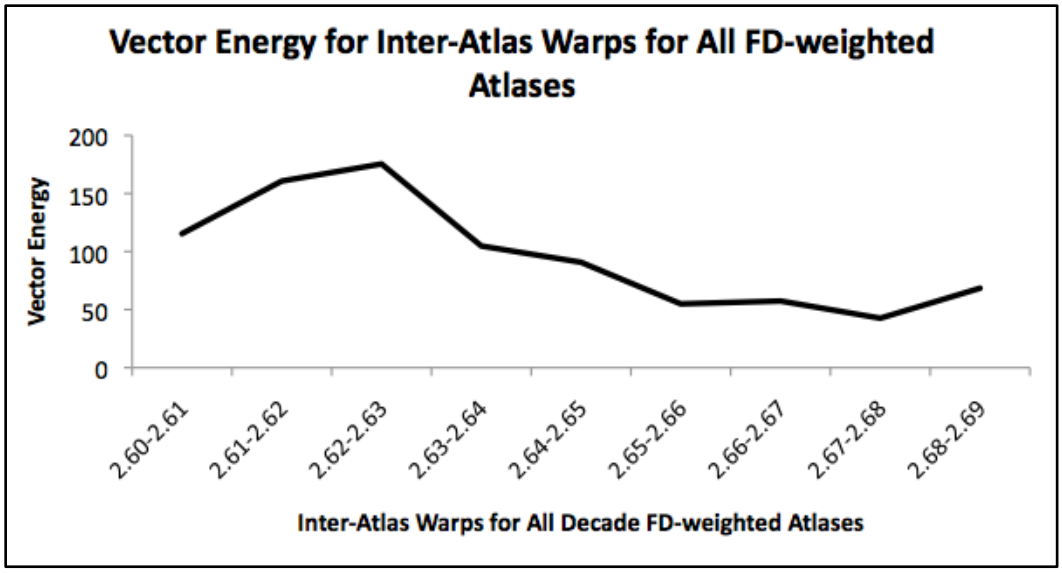

Figure 4.9 Interatlas analysis of FD-weighted atlases. Amount of vector energy it takes to deform each global fractal dimension-weighted atlas to the successive atlas has been plotted. A significant difference was found in the amount of vector energy it takes to deform each image to its respective atlas from 2.61-2.62, 2.62-2.63, 2.63-2.64, 2.64-2.65, 2.65-2.66, 2.66-2.67, & 2.68-2.69.

Table 4.1 Student's t-test for half-decades. Student's t-test (2 tailed, model 3) to compare the amount of vector energy to deform each image to its respective atlas for successive half-decade atlases was performed. There was significant difference in the amount of vector energy it takes to deform each image to its respective atlas from 55-60, 60-65, 65-70, & 75-80.

2-tailed T-Test for Vector Energies for All Half-decade Age-weighted Atlases

Compared Age Groups	p-value
20-25	0.9121246
25-30	0.7456880
30-35	0.8338176
35-40	0.1948091
40-45	0.3843492
45-50	0.3803742
50-55	0.3137866
55-60	0.0000712
60-65	0.0308956
65-70	0.0126778
70-75	0.1351103
75-80	0.0143392
80-85	0.0852710

Table 4.2 Student's t-test for decades. Student's t-test (2 tailed, model 3) to compare the amount of vector energy to deform each image to its respective atlas for successive decade atlases has been performed. Significant differences ($p < 0.05$) have been highlighted in yellow. We found similar results as the aforementioned half-decade analysis.

2-tailed T-Test for Vector Energies for All Decade Age-weighted Atlases

Compared Age Groups	p-value
20-30	0.6671726
30-40	0.2863876
40-50	0.0717665
50-60	0.0000089
60-70	0.0000143
70-80	0.0000038

Table 4.3 Student's t-test for two-decades. Student's t-test (2 tailed, model 3) to compare the amount of vector energy to deform each image to its respective atlas for successive two-decade atlases has been performed. Significant differences ($p < 0.05$) have been highlighted in yellow. Significant difference in the amount of vector energy it takes to deform each image to its respective atlas from 30-50, 40-60, 50-70, & 60-80 was found.

2-tailed T-Test for Vector Energies for All Two-decade Age-weighted Atlases

Compared Age Groups	p-value
20-40	0.6530164
30-50	0.0095888
40-60	0.0000000
50-70	0.0000000
60-80	0.0000000

Table 4.4 Student's t-test with Atlas 20 as gold standard. Student's t-test (2 tailed, model 3) to compare the vector energy required for each image in Atlas 20 to be deformed to the Atlas 20 image as compared to the vector energy required for each image to be deformed to its respective half-decade atlas (top) and decade-atlas (bottom). Significant differences ($p < 0.05$) have been highlighted in yellow. A significant difference was found in the shape of the cerebral cortex between the atlases from age 55 onwards for the analysis with half-decades and from age 60 onwards for the analysis with decades.

2-tailed T-Test for Vector Energies for Age-weighted Atlas of 20 year-olds (gold standard) and All Half-decade Age-weighted Atlases

Compared Age Groups	p-value
20-25	0.9121246
20-30	0.6671726
20-35	0.5388033
20-40	0.6530164
20-45	0.2733215
20-50	0.0734277
20-55	0.0095501
20-60	0.0000002
20-65	0.0000000
20-70	0.0000000
20-75	0.0000000
20-80	0.0000000
20-85	0.0000000

2-tailed T-Test for Vector Energies for Age-weighted Atlas of 20 year-olds (gold standard) and All Decade Age-weighted Atlases

Compared Age Groups	p-value
20-30	0.6671726
20-40	0.6530164
20-50	0.0734277
20-60	0.0000002
20-70	0.0000000
20-80	0.0000000

CHAPTER 5

CHARACTERIZATION OF SPATIOTEMPORAL CHANGES IN SHAPE COMPLEXITY OF THE CEREBRAL CORTEX ON A LOBAR AND REGIONAL SCALE ACROSS THE ADULT HUMAN LIFESPAN

5.1 Abstract

Advances in postimaging analysis of human brain MR images have enabled the quantification of fractal dimension (a measure of shape complexity) on the human cerebral cortex at a local level. The purpose of this paper is to characterize the spatiotemporal distribution of changes in cortical fractal dimension on a lobar and regional scale across the adult human lifespan in a large, healthy, cross-sectional database (N=301, age range: 20-88).

High-contrast MR scans (MP-RAGE format) were downloaded from the Dallas Lifespan Brain Study. Each scan was processed using FreeSurfer to semiautomatically generate a cortical/subcortical segmentation and cortical parcellation. Cortical labels were applied by FreeSurfer based upon the

Desikan-Killiany atlas. The fractal dimension for a 30mm local region was computed independently for every cortical voxel using custom software (C^3). The cortical labels were aligned with the fractal dimension maps, and aggregate statistics on regions of interest were generated using a MATLAB script.

A linear decrease in cerebral cortical complexity across the adult human lifespan at both the lobar- and regional-level was observed. Variable effects on the cerebral cortex, with some regions being more selectively prone to age-related atrophy, varied across age ranges. On the regional level, the inferior temporal, inferior parietal, lateral occipital, middle temporal, entorhinal, fusiform, and temporal pole regions of the left hemisphere had the least amount of change in cortical complexity across the adult human lifespan. In contrast, the superior frontal, isthmus cingulate, posterior cingulate, and lingual regions had the greatest amount of change in cortical complexity across the adult human lifespan.

This study highlights the variable effects of normal aging on the cerebral cortex based upon local complexity changes. Having established this reference of normal could serve as important comparative biomarker when trying to identify individuals at risk for disease, such as Alzheimer's disease, that are known to affect cortical complexity.

5.2 Introduction

The structure of the human cerebral cortex undergoes significant changes throughout the adult lifespan. Even in the absence of any measurable or symptomatic cerebral disease, there are measurable changes in the properties of the cerebral cortex (e.g., thickness, volume, curvature, gyrification index, complexity). Numerous studies have documented volumetric and shape changes. These studies of normal aging can serve as reference biomarkers when trying to distinguish the effects of normal aging from those of progressive neurodegenerative disease.

In a recent large study of normal aging, global fractal dimension (a measure of shape complexity) was recently found to steadily decrease across the lifespan in healthy individuals aged 20-89, as seen in Chapter 3. However, it is also clear that normal aging (and neurodegenerative diseases) have variable effects on the cerebral cortex, with some regions being more selectively prone to age-related atrophy [1-3]. Additionally, several groups have reported on the acceleration of atrophy with normal aging for particular regions [1,4-6]. Given that cortical atrophy is a focal process, additional information will be gained by performing the characterization of cortical complexity changes due to normal aging at a local scale.

Another motivation is that the local pattern of cortical complexity loss with aging differs from alterations associated with neurodegenerative disease, such as Alzheimer's disease or Frontotemporal dementia. A robust

analysis at a local scale will lead to the characterization of spatial and temporal pattern signatures of cerebral cortical fractal dimension associated with normal aging and our understanding of the patterns and trajectories of change with normal aging will help us to characterize change with neurodegenerative diseases, without the effects of normal aging, better.

Advances in postimaging analysis have enabled the ability to compute the fractal cerebral dimension of the cortex on a local region of predefined size. The value for a region of interest can then be calculated by aggregating individual values of all cortical voxels that share a particular property (i.e., are contained in a particular lobe, or are located in a particular gyrus). The labels of the cerebral cortex are generated using semiautomatic cortical segmentation and parcellation software (FreeSurfer).

The purpose of this paper is to characterize local cerebral cortical complexity changes on a lobar and ROI level and to report on the laterality, linearity, and spatiotemporal distribution of change in the shape complexity of the cerebral cortex across the adult human lifespan, by a large cross-sectional examination.

5.3 Methodology

5.3.1 Participants

Participants for this study were 301 individuals aged 20-88 (mean 52.8 ± 19.6 years; uniform age distribution with ~44 subjects per decade; 192

women, 109 men) from the Dallas Lifespan Brain Study. For more information on DLBS see Chapter 3, Sections 3.3.1 and 3.3.2.

5.3.2 MRI Acquisition

All participants were scanned on a single 3T Philips Achieva scanner equipped with an 8-channel head coil. High-resolution anatomical images were collected with a T1-weighted MP-RAGE sequence with 160 sagittal slices, 1×1×1mm^3 voxel; 204×256×160 matrix, TR=8.1ms, TE=3.7ms, flip-angle=12°. The raw data used in this study were extracted from high-resolution high contrast magnetic resonance images (MP-RAGE, resolution of 1 x 1 x 1.25mm, TR =9.7 ms, TE= 4 ms, flip angle = 10 degrees, T1 = 20 msec, and TD = 200 msec).

5.3.3 MRI Processing

Segmentation of the brain images was performed using a semiautomated segmentation software suite called FreeSurfer (Athinoula A. Martinos Center for Biomedical Imaging, Massachusetts General Hospital, Boston). FreeSurfer contains a set of tools for analysis and visualization of structural and functional brain imaging data. FreeSurfer has been described in detail in prior publications [9-17] and our pipeline for image segmentation with FreeSurfer with subsequent manual editing has been described in Chapter 3.

The cortical parcellation is created by labeling each cortical voxel based on registration to a spherical atlas [18]. By the parcellation of the cerebral cortex into units with respect to gyral and sulcal structure [13,19] cortical parcellation regions for each hemisphere were identified.

5.3.4 Computing Local Fractal Dimension

The fractal dimension (FD) of the cortical ribbon was computed using a custom software program called the Cortical Complexity Calculator. The version of C^3 used in this study was written on Mac OS X (10.5) using the XCode environment in Objective C with graphic implementation using OpenGL. Computation of local fractal dimension has been described in Chapter 2.

The cortical parcellation image generated by FreeSurfer was then co-registered with the local fractal dimension image using a MATLAB script. To compute regional values for each cortical region, for each hemisphere, we grouped all cortical voxels that shared the same parcellation label as determined by FreeSurfer. The regions were then grouped to form larger regions (lobes) based upon the FreeSurfer predetermined scheme.

5.4 Results

5.4.1 Lobar Results

For both hemispheres, the mean fractal dimension of the lobes across the lifespan was consistently in the following order: temporal > occipital > parietal > frontal. The average data for subjects in their 20s and 80s are summarized in Table 5.1. Fractal dimension values for each lobe (Frontal, Parietal, Temporal, and Occipital) for both left and right hemispheres for all subjects in this study are shown in Figure 5.1.

There is a linear decrease in fractal dimension across the lifespan for all the lobes. The normalized percent difference between the 20s and 80s cohort ranged from 18.1% (Left frontal) to 11.5% (Right occipital). The rate of change of fractal dimension across the lifespan of the lobes, for both hemispheres, followed the following order: frontal > parietal > temporal > occipital. For all lobes, the change in cortical fractal dimension between the 20s and 80s cohorts were statistically significant ($p < 0.001$).

As seen in Figure 5.2, there is consistent asymmetry between the hemispheres with the left having a greater fractal dimension that the right. The difference between all lobes was statistically significant ($p < 0.0001$). The degree of asymmetry does not change significantly over the lifespan (20s vs. 80s: Frontal $p = 0.108$; Parietal $p = 0.937$; Temporal $p = 0.377$; Occipital $p = 0.698$). The Frontal lobe showed the smallest inter-hemispheric difference in fractal dimension (6.7%). The Parietal and Temporal lobes were the most

asymmetric with a normalized percent difference of 14.1%. The Occipital lobes measured an 11.1% difference between left and right hemispheres. The variance of the difference in mean lobar fractal dimension between the left and right hemispheres was in the following order: Occipital > Temporal > parietal > Frontal.

5.4.2 ROI Results

5.4.2.1 Changes Across the Regions

The change in fractal dimension for all subject in 30 of the 35 parcellated cortical regions are shown in Figure 5.3 (left hemisphere only), and the data for the 20s and 80s cohorts (both hemispheres) are summarized in Table 5.2.

Similar to the lobar data, there was a linear decrease in cortical fractal dimension for all regions. There change in fractal dimension between the 20s cohort and the 80s cohort was statistically significant for all of the regions of the cortex ($p < 0.001$). The amount of change that occurred with normal aging varied from 22.7% (L. superior frontal gyrus) to 8.1% (L. middle temporal gyrus). This difference in fractal dimension was found to be bilaterally high in the superior frontal (3I: A), isthmus cingulate (3II: D), posterior cingulate (3II: F), and lingual regions (3II: B) of the cortex. In contrast, this difference in fractal dimension was found to be low in the inferior temporal (3I: O), inferior parietal (3I: H), lateral occipital (3I: P), middle temporal (3I: N),

entorhinal (3II: M), fusiform (3II: K), and temporal pole (3II: N) regions. The degree of change across the lifespan was not significantly different between left and right hemispheres for all regions of interest.

Certain regions of interest (ROIs) have higher baseline fractal dimension than other ROIs. The middle temporal (3I: N), inferior temporal (3I: O), superior temporal (3I: M), lateral occipital (3I: P), and inferior parietal (3I: H) regions of the left hemisphere and the entorhinal (3II: M) region of the right hemisphere had the highest baseline fractal dimension (~ 2.83 – 2.85). The mean fractal dimension of the cuneus (3II: A) was bilaterally high (~ 2.80). In contrast, the pars orbitalis (3I: J), rostral middle frontal (3I: B), caudal middle frontal (3I: C), and precentral (3I: D) regions of the right hemisphere and the parahippocampal (3II: L) region of the left hemisphere had the lowest mean fractal dimension (~ 2.68- 2.70). The mean fractal dimension of the frontal pole (3II: J) was bilaterally low (2.68 -2.69). The rate of change of fractal dimension across the lifespan is higher for certain ROIs. The regions that showed the greatest change in average decade-cohort values between the 20s and the 80s were the superior frontal (3I:A), para-central (3II:E), and pre-central (3I:D) gyri bilaterally (normalized % difference 19.2 - 22.7). The smallest percent change was seen in the inferior temporal (3I: O), middle temporal (3I: N), and lateral occipital (3I:P) regions of the cortex (8.1 – 10.9%).

Certain ROIs have a higher variance of fractal dimension than others, as can be seen in Figure 5.3. The variance of fractal dimension was bilaterally high in the parahippocampal (3II: L), entorhinal (3II: M), and temporal pole (3II: N) regions of the cortex. In contrast, the variance of fractal dimension was bilaterally low in the middle temporal (3I: N), rostral middle frontal (3I: B), and precuneus (3II: C) regions of the cortex. The variance of fractal dimension was unilaterally low in the suporamarginal (3I: F) and inferior parietal (3I: H) regions of the right hemisphere.

5.4.2.2 Changes Between Hemispheres:

Left versus Right

The left hemisphere dominant asymmetry that we found at the lobar-level has been validated at the regional level, as well (Figure 5.4). With a couple exceptions, the fractal dimension of all the regions were found to be significantly higher on the left. The exception are the lingual (4II:B), fusiform, parahippocampal, entorhinal, and temporal pole regions where are significantly larger on the right hemisphere, and the cuneus (4II: A) and medial orbitofrontal (4II: I) regions of the cortex which are not significantly different from left to right. Furthermore, we did not find significant change in the degree of asymmetry across the lifespan for any region.

5.4.2.3 Changes Between Surfaces:

Lateral versus Medial

The mean and rate of change of fractal dimension for all the regions of the lateral and medial surfaces were not found to be significantly different. However, the difference in fractal dimension of the youngest subject (20-year-old) and oldest subject (88-year-old) and variance of fractal dimension for all the regions of the lateral and medial surfaces were found to be significantly different.

5.5 Discussion

To the best of our knowledge, this is the first large, cross-sectional study to report on quantitative characterization of lobar and regional changes in cerebral cortical complexity through the adult human lifespan for a cognitively normal population. Several groups have determined that age-related changes of other measures vary regionally. However, the findings in the existing literature is mixed in the evolution of these changes, in terms of linearity, laterality, etc., across the human lifespan. The conflicted nature of results of the previous studies may be due to difference in the sample groups [20], i.e., sample size, age range, handedness, or differences in data acquisition and processing [21], i.e., modality, scanning parameters, software, segmentation methods.

We have found a linear decrease in cerebral cortical complexity across the adult human lifespan at both lobar and regional levels. There are several groups that have reported a linear change with other measures, such as cortical thickness [4,22] and volumetric measures [23-25] with age. However, other groups have reported a nonlinear change with measures, such as voxel-based morphometry [26,27] gray matter density [28] cortical thickness [29] and volumetric measures [1,23,30-34] with age.

In regards to laterality, it is generally accepted that the brain hemispheres are anatomically and functionally asymmetric and changes in asymmetry have been linked to the gain or loss of cognitive traits [35-37] and [38,39]. Our findings on a lobar level indicate that the left hemisphere has a higher cortical complexity than the right hemisphere. For a few individuals, the right hemisphere had a higher cortical complexity than the left hemisphere for the occipital lobe. Upon inspection, there was a clear visible asymmetry with the left hemisphere being smaller than the right side. The clinical significance of this is unclear, as all individuals in the study performed at normal cognitive levels. Despite the larger right cerebrum, these individuals still reported being right-handed (left hemisphere dominant).

The overall left hemisphere dominant asymmetry in our findings aligns with the functional right hemi-aging hypothesis, which states that age-related cognitive decline affects the right hemisphere to a greater degree than

the left hemisphere [40]. Several groups have demonstrated this left hemisphere dominant asymmetry at specific regions with other measures, such as cortical thickness [29,38,41,42] and cortical connectivity [43]. Other groups have found a right hemisphere dominant asymmetry in other regions in cortical thickness [29] and volumetric studies [44]. Furthermore, the variance of the difference in mean lobar fractal dimension between the left and right hemispheres was in the following order: occipital > temporal > parietal > frontal.

We found that there is no significant change in the degree of asymmetry across the lifespan. This finding is in contrast to findings from other groups of the degree of asymmetry changing across the lifespan and across different regions [29,45], particularly decreasing with age [46-49].

A key limitation to such studies is that brain asymmetry and handedness are interrelated in a complex way [50,51]. In this study, the participants were strongly right-handed as determined by the Edinburgh Handedness Questionnaire. Therefore, these results may not be applicable to left-handed individuals. To explore the evolution of age-related changes across the lifespan, all potential confounders that affect brain asymmetry, such as handedness, neuropsychological state, sex, and environmental-brain interaction [52-55], need to be accounted for. For example, other groups have demonstrated that measures such as sex [29,56] and IQ [57-60] significantly moderate brain symmetry. It should be noted that groups have also shown

sex to not have a significant difference in brain asymmetry [45,41,61,62].

Another limitation to the interpretation of our results is that this is a cross-sectional study and assumptions of age-related trends ignore possible sampling biases, cohort effects, and developmental histories of the participants. Longitudinal studies with large samples and wide age ranges would be better to explore age-related changes.

5.6 Conclusions

This study demonstrates that application of fractal dimension techniques to the cerebral cortex on a lobar and regional scale, rather than on a global scale, can provide additional insight into the spatiotemporal pattern of shape change of the cerebral cortex with the normal aging process. Additionally, the application of these techniques to develop spatiotemporal patterns of shape change of the cortex for neurodegenerative diseases may help improve the dissociation of changes related with normal aging from changes associated with each disease, in an effort to ultimately continue to improve the standard of care of patients with neurodegenerative diseases.

5.7 Acknowledgements

I thank Drs. Norman Foster, P. Thomas Fletcher, Alan Dorval, Sarang Joshi, and Angela Wang for constructive discussions related to and support of this work. Also, I thank Carena Kole and Drs. Denise Park and Richard King

for their contributions to this study. Finally, I thank Benjamin Tyler for his assistance on this study.

This project was supported by the Center for Alzheimer's Care Imaging and Research at the University of Utah, and grants from the Robert Wood Johnson Foundation, National Institute of Aging (5-R37-AG006265-27, 5-P30-AG012300-15, and K23-AG03835), and the Alzheimer's Association.

5.8 References

[1] N. Raz, "Regional brain changes in aging healthy adults: general trends, individual differences and modifiers," Cerebral Cortex, vol. 15, no. 11, pp. 1676-1689, 2005.

[2] N. Raz, P. Ghisletta, K. Rodrigue, K. Kennedy and U. Lindenberger, "Trajectories of brain aging in middle-aged and older adults: regional and individual differences," NeuroImage, vol. 51, no. 2, pp. 501-511, 2010.

[3] K. Walhovd, L. Westlye, I. Amlien, T. Espeseth, I. Reinvang, N. Raz, I. Agartz, D. Salat, D. Greve, B. Fischl, A. Dale and A. Fjell, "Consistent neuroanatomical age-related volume differences across multiple samples," Neurobiology of Aging, vol. 32, no. 5, pp. 916-932, 2011.

[4] A. Fjell, L. Westlye, I. Amlien, T. Espeseth, I. Reinvang, N. Raz, I. Agartz, D. Salat, D. Greve, B. Fischl, A. Dale and K. Walhovd, "High consistency of regional cortical thinning in aging across multiple samples," Cerebral Cortex, vol. 19, no. 9, pp. 2001-2012, 2009.

[5] I. Driscoll, C. Davatzikos, Y. An, X. Wu, D. Shen, M. Kraut and S. Resnick, "Longitudinal pattern of regional brain volume change differentiates normal aging from MCI," Neurology, vol. 72, no. 22, pp. 1906-1913, 2009.

[6] R. Scahill, C. Frost, R. Jenkins, J. Whitwell, M. Rossor and N. Fox, "A Longitudinal study of brain volume changes in normal aging using serial registered magnetic resonance imaging," Arch Neurol, vol. 60, no. 7, p. 989, 2003.

[7] R. Oldfield, "The assessment and analysis of handedness: the Edinburgh inventory," Neuropsychologia, vol. 9, no. 1, pp. 97-113, 1971.

[8] M. F. Folstein, S. E. Folstein, P. R. McHugh, "Mini-mental state: a practical method for grading the cognitive state of patients for the clinician," Journal of psychiatric research, vol. 12, no. 3, pp. 189-198, 1975.

[9] B. Fischl, "FreeSurfer," Neuroimage, vol. 62, no. 2, pp. 774-781, 2012.

[10] A. Dale, B. Fischl and M. Sereno, "Cortical surface-based analysis," NeuroImage, vol. 9, no. 2, pp. 179-194, 1999.

[11] B. Fischl, A. Liu and A. Dale, "Automated manifold surgery: constructing geometrically accurate and topologically correct models of the human cerebral cortex," IEEE Transactions on Medical Imaging, vol. 20, no. 1, pp. 70-80, 2001.

[12] B. Fischl, D. Salat, E. Busa, M. Albert, M. Dieterich, C. Haselgrove, A. van der Kouwe, R. Killiany, D. Kennedy, S. Klaveness, A. Montillo, N. Makris, B. Rosen and A. Dale, "Whole brain segmentation," Neuron, vol. 33, no. 3, pp. 341-355, 2002.

[13] B. Fischl, "Automatically parcellating the human cerebral cortex," Cerebral Cortex, vol. 14, no. 1, pp. 11-22, 2004.

[14] X. Han, J. Jovicich, D. Salat, A. van der Kouwe, B. Quinn, S. Czanner, E. Busa, J. Pacheco, M. Albert, R. Killiany, P. Maguire, D. Rosas, N. Makris, A. Dale, B. Dickerson and B. Fischl, "Reliability of MRI-derived measurements of human cerebral cortical thickness: the effects of field strength, scanner upgrade and manufacturer," NeuroImage, vol. 32, no. 1, pp. 180-194, 2006.

[15] J. Jovicich, S. Czanner, D. Greve, E. Haley, A. van der Kouwe, R. Gollub, D. Kennedy, F. Schmitt, G. Brown, J. MacFall, B. Fischl and A. Dale, "Reliability in multi-site structural MRI studies: effects of gradient non-linearity correction on phantom and human data," NeuroImage, vol. 30, no. 2, pp. 436-443, 2006.

[16] F. Segonne, J. Pacheco and B. Fischl, "Geometrically accurate topology-correction of cortical surfaces using nonseparating loops,"

IEEE Transactions on Medical Imaging, vol. 26, no. 4, pp. 518-529, 2007.

[17] B. Fischl and A. Dale, "Measuring the thickness of the human cerebral cortex from magnetic resonance images," Proceedings of the National Academy of Sciences, vol. 97, no. 20, pp. 11050-11055, 2000.

[18] B. Fischl, M. Sereno, R. Tootell and A. Dale, "High-resolution intersubject averaging and a coordinate system for the cortical surface," Human Brain Mapping, vol. 8, no. 4, pp. 272-284, 1999.

[19] R. Desikan, F. Ségonne, B. Fischl, B. Quinn, B. Dickerson, D. Blacker, R. Buckner, A. Dale, R. Maguire, B. Hyman, M. Albert and R. Killiany, "An automated labeling system for subdividing the human cerebral cortex on MRI scans into gyral based regions of interest," NeuroImage, vol. 31, no. 3, pp. 968-980, 2006.

[20] M. Cykowski, O. Coulon, P. Kochunov, K. Amunts, J. Lancaster, A. Laird, D. Glahn and P. Fox, "The central sulcus: an observer-independent characterization of sulcal landmarks and depth asymmetry," Cerebral Cortex, vol. 18, no. 9, pp. 1999-2009, 2007.

[21] V. Kovalev, F. Kruggel and D. von Cramon, "Gender and age effects in structural brain asymmetry as measured by MRI texture analysis," NeuroImage, vol. 19, no. 3, pp. 895-905, 2003.

[22] A. Fjell, L. Westlye, H. Grydeland, I. Amlien, T. Espeseth, I. Reinvang, N. Raz, A. Dale and K. Walhovd, "Accelerating cortical thinning: unique to dementia or universal in aging?," Cerebral Cortex, vol. 24, no. 4, pp. 919-934, 2012.

[23] N. Raz, F. Gunning-Dixon, D. Head, K. Rodrigue, A. Williamson and J. Acker, "Aging, sexual dimorphism, and hemispheric asymmetry of the cerebral cortex: replicability of regional differences in volume," Neurobiology of Aging, vol. 25, no. 3, pp. 377-396, 2004.

[24] N. Raz, "Selective aging of the human cerebral cortex observed in vivo: differential vulnerability of the prefrontal gray matter," Cerebral Cortex, vol. 7, no. 3, pp. 268-282, 1997.

[25] E. Courchesne, H. Chisum, J. Townsend, A. Cowles, J. Covington, B. Egaas, M. Harwood, S. Hinds and G. Press, "Normal brain development and aging: quantitative analysis at in vivo MR imaging in healthy volunteers," Radiology, vol. 216, no. 3, pp. 672-682, 2000.

[26] G. Ziegler, R. Dahnke, L. Jäncke, R. Yotter, A. May and C. Gaser, "Brain structural trajectories over the adult lifespan," Human Brain Mapping, vol. 33, no. 10, pp. 2377-2389, 2011.

[27] K. Kennedy, K. Erickson, K. Rodrigue, M. Voss, S. Colcombe, A. Kramer, J. Acker and N. Raz, "Age-related differences in regional brain volumes: a comparison of optimized voxel-based morphometry to manual volumetry," Neurobiology of Aging, vol. 30, no. 10, pp. 1657-1676, 2009.

[28] E. Sowell, B. Peterson, P. Thompson, S. Welcome, A. Henkenius and A. Toga, "Mapping cortical change across the human life span," Nature Neuroscience, vol. 6, no. 3, pp. 309-315, 2003.

[29] K. Plessen, K. Hugdahl, R. Bansal, X. Hao and B. Peterson, "Sex, age, and cognitive correlates of asymmetries in thickness of the cortical mantle across the life span," Journal of Neuroscience, vol. 34, no. 18, pp. 6294-6302, 2014.

[30] J. Allen, J. Bruss, C. Brown and H. Damasio, "Normal neuroanatomical variation due to age: the major lobes and a parcellation of the temporal region," Neurobiology of Aging, vol. 26, no. 9, pp. 1245-1260, 2005.

[31] P. Curiati, J. Tamashiro, P. Squarzoni, F. Duran, L. Santos, M. Wajngarten, C. Leite, H. Vallada, P. Menezes, M. Scazufca, G. Busatto and T. Alves, "Brain structural variability due to aging and gender in cognitively healthy elders: results from the Sao Paulo Ageing and Health Study," American Journal of Neuroradiology, vol. 30, no. 10, pp. 1850-1856, 2009.

[32] D. Terribilli, M. Schaufelberger, F. Duran, M. Zanetti, P. Curiati, P. Menezes, M. Scazufca, E. Amaro, C. Leite and G. Busatto, "Age-related gray matter volume changes in the brain during non-elderly adulthood," Neurobiology of Aging, vol. 32, no. 2, pp. 354-368, 2011.

[33] A. Fjell, L. Westlye, H. Grydeland, I. Amlien, T. Espeseth, I. Reinvang, N. Raz, D. Holland, A. Dale and K. Walhovd, "Critical ages in the life course of the adult brain: nonlinear subcortical aging," Neurobiology of Aging, vol. 34, no. 10, pp. 2239-2247, 2013.

[34] N. Schuff, D. Tosun, P. Insel, G. Chiang, D. Truran, P. Aisen, C. Jack and M. Weiner, "Nonlinear time course of brain volume loss in

cognitively normal and impaired elders," Neurobiology of Aging, vol. 33, no. 5, pp. 845-855, 2012.

[35] M. Herbert, "Brain asymmetries in autism and developmental language disorder: a nested whole-brain analysis," Brain, vol. 128, no. 1, pp. 213-226, 2004.

[36] S. Illingworth and D. Bishop, "Atypical cerebral lateralisation in adults with compensated developmental dyslexia demonstrated using functional transcranial Doppler ultrasound," Brain and Language, vol. 111, no. 1, pp. 61-65, 2009.

[37] E. Luders, C. Gaser, L. Jancke and G. Schlaug, "A voxel-based approach to gray matter asymmetries," NeuroImage, vol. 22, no. 2, pp. 656-664, 2004.

[38] P. Shaw, F. Lalonde, C. Lepage, C. Rabin, K. Eckstrand, W. Sharp, D. Greenstein, A. Evans, J. Giedd and J. Rapoport, "Development of cortical asymmetry in typically developing children and its disruption in Attention-Deficit/Hyperactivity Disorder," Arch Gen Psychiatry, vol. 66, no. 8, p. 888, 2009.

[39] J. H. Kim, J. W. Lee, G. H. Kim, J. H. Roh, M. J. Kim, S. W. Seo, D. L. Na, "Cortical asymmetries in normal, mild cognitive impairment, and Alzheimer's disease," Neurobiology of aging, vol. 33, no. 9, 2012.

[40] J. Brown and J. Jaffe, "Hypothesis on cerebral dominance," Neuropsychologia, vol. 13, no. 1, pp. 107-110, 1975.

[41] E. Luders, "Hemispheric asymmetries in cortical thickness," Cerebral Cortex, vol. 16, no. 8, pp. 1232-1238, 2005.

[42] L. Wang, M. Hosakere, J. Trein, A. Miller, J. Ratnanather, D. Barch, P. Thompson, A. Qiu, M. Gado, M. Miller and J. Csernansky, "Abnormalities of cingulate gyrus neuroanatomy in schizophrenia," Schizophrenia Research, vol. 93, no. 1-3, pp. 66-78, 2007.

[43] L. Bonilha, T. Nesland, C. Rorden and J. Fridriksson, "Asymmetry of the structural brain connectome in healthy older adults," Frontiers in Psychiatry, vol. 4, 2014.

[44] R. Carne, S. Vogrin, L. Litewka and M. Cook, "Cerebral cortex: An MRI-based study of volume and variance with age and sex," Journal of Clinical Neuroscience, vol. 13, no. 1, pp. 60-72, 2006.

[45] D. Zhou, C. Lebel, A. Evans and C. Beaulieu, "Cortical thickness asymmetry from childhood to older adulthood," NeuroImage, vol. 83, pp. 66-74, 2013.

[46] R. Cabeza, "Hemispheric asymmetry reduction in older adults: the HAROLD model.," Psychology and Aging, vol. 17, no. 1, pp. 85-100, 2002.

[47] R. Cabeza, "Task-independent and task-specific age effects on brain activity during working memory, visual attention and episodic retrieval," Cerebral Cortex, vol. 14, no. 4, pp. 364-375, 2004.

[48] N. Dennis, H. Kim and R. Cabeza, "Effects of aging on true and false memory formation: an fMRI study," Neuropsychologia, vol. 45, no. 14, pp. 3157-3166, 2007.

[49] Z. Li, A. Moore, C. Tyner and X. Hu, "Asymmetric connectivity reduction and its relationship to "HAROLD" in aging brain," Brain Research, vol. 1295, pp. 149-158, 2009.

[50] E. Koff, M. Naeser, J. Pieniadz, A. Foundas and H. Levine, "Computed tomographic scan hemispheric asymmetries in right- and left-handed male and female Subjects," Archives of Neurology, vol. 43, no. 5, pp. 487-491, 1986.

[51] S. Dos Santos Sequeira, W. Woerner, C. Walter, F. Kreuder, U. Lueken, R. Westerhausen, R. Wittling, E. Schweiger and W. Wittling, "Handedness, dichotic-listening ear advantage, and gender effects on planum temporale asymmetry—a volumetric investigation using structural magnetic resonance imaging," Neuropsychologia, vol. 44, no. 4, pp. 622-636, 2006.

[52] M. Hirnstein, S. Leask, J. Rose and M. Hausmann, "Disentangling the relationship between hemispheric asymmetry and cognitive performance," Brain and Cognition, vol. 73, no. 2, pp. 119-127, 2010.

[53] S. E. Nadeau, "Hemispheric asymmetry: What, why, and at what cost?," Journal of the International Neuropsychological Society, vol. 16, no. 4, pp. 593, 2010.

[54] T. Sun and C. Walsh, "Molecular approaches to brain asymmetry and handedness," Nature Reviews Neuroscience, vol. 7, no. 8, pp. 655-662, 2006.

[55] L. Tian, J. Wang, C. Yan and Y. He, "Hemisphere- and gender-related differences in small-world brain networks: a resting-state functional MRI study," NeuroImage, vol. 54, no. 1, pp. 191-202, 2011.

[56] B. Crespo-Facorro, R. Roiz-Santiáñez, R. Pérez-Iglesias, I. Mata, J. Rodríguez-Sánchez, D. Tordesillas-Gutiérrez, V. Ortíz-García de la Foz, R. Tabarés-Seisdedos, E. Sánchez, N. Andreasen, V. Magnotta and J. Vázquez-Barquero, "Sex-specific variation of MRI-based cortical morphometry in adult healthy volunteers: the effect on cognitive functioning," Progress in Neuro-Psychopharmacology and Biological Psychiatry, vol. 35, no. 2, pp. 616-623, 2011.

[57] Y. Choi, N. Shamosh, S. Cho, C. DeYoung, M. Lee, J. Lee, S. Kim, Z. Cho, K. Kim, J. Gray and K. Lee, "Multiple bases of human intelligence revealed by cortical thickness and neural activation," Journal of Neuroscience, vol. 28, no. 41, pp. 10323-10329, 2008.

[58] S. Frangou, X. Chitins and S. Williams, "Mapping IQ and gray matter density in healthy young people," NeuroImage, vol. 23, no. 3, pp. 800-805, 2004.

[59] K. Narr, R. Woods, P. Thompson, P. Szeszko, D. Robinson, T. Dimtcheva, M. Gurbani, A. Toga and R. Bilder, "Relationships between IQ and regional cortical gray matter thickness in healthy adults," Cerebral Cortex, vol. 17, no. 9, pp. 2163-2171, 2006.

[60] P. Shaw, D. Greenstein, J. Lerch, L. Clasen, R. Lenroot, N. Gogtay, A. Evans, J. Rapoport and J. Giedd, "Intellectual ability and cortical development in children and adolescents," Nature, vol. 440, no. 7084, pp. 676-679, 2006.

[61] L. Hamilton, K. Narr, E. Luders, P. Szeszko, P. Thompson, R. Bilder and A. Toga, "Asymmetries of cortical thickness: effects of handedness, sex, and schizophrenia," NeuroReport, vol. 18, no. 14, pp. 1427-1431, 2007.

[62] E. Sowell, B. Peterson, E. Kan, R. Woods, J. Yoshii, R. Bansal, D. Xu, H. Zhu, P. Thompson and A. Toga, "Sex differences in cortical thickness mapped in 176 healthy individuals between 7 and 87 Years of age," Cerebral Cortex, vol. 17, no. 7, pp. 1550-1560, 2006.

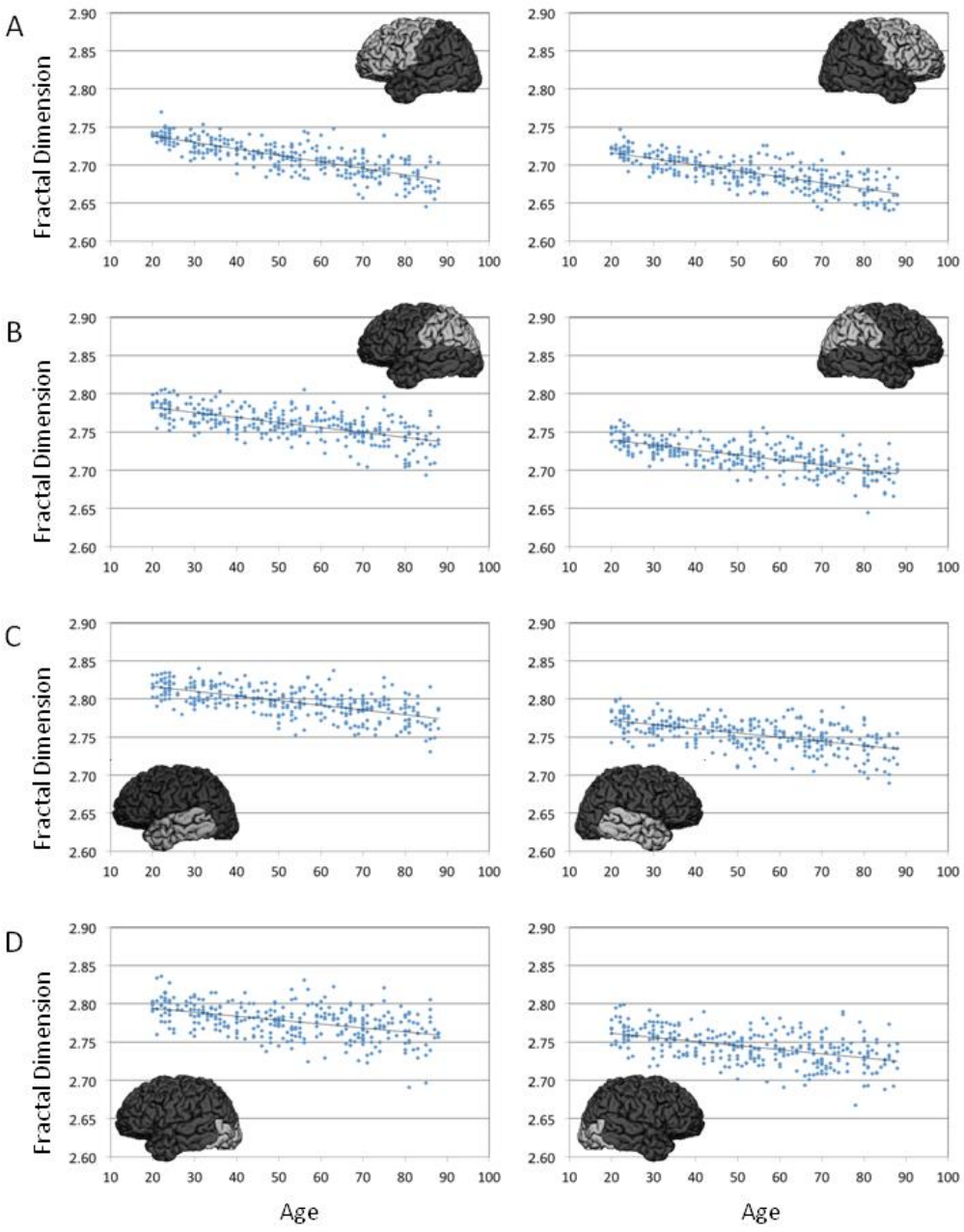

Figure 5.1 Fractal dimension on a lobar scale across the lifespan. The blue dots show the fractal dimension of a given lobe for each of the 301 subjects in this study. The left column shows the left hemisphere lobes, and the right column shows the right hemisphere. **A.** frontal lobe **B**. parietal lobe **C.** temporal lobe **D**. occipital lobe. All lobes showed a linear decrease in fractal dimension with age.

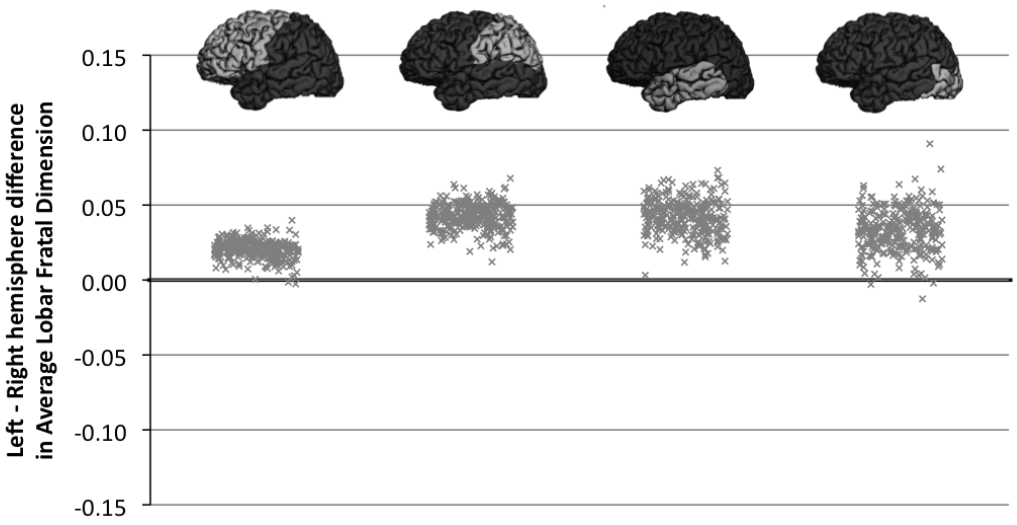

Figure 5.2 Asymmetry in lobar fractal dimension. The individual differences in fractal dimension between the lobes of the left and right hemisphere are shown for the frontal, parietal, temporal, and occipital lobes (from left to right). Within each lobe, the subjects are displayed in order of age. In general, the left hemisphere has a higher complexity than the right hemisphere in this population. The degree of asymmetry does not change significantly with age. The frontal lobe tended to be the least asymmetric, whereas there is considerably more variance in the occipital lobe asymmetry.

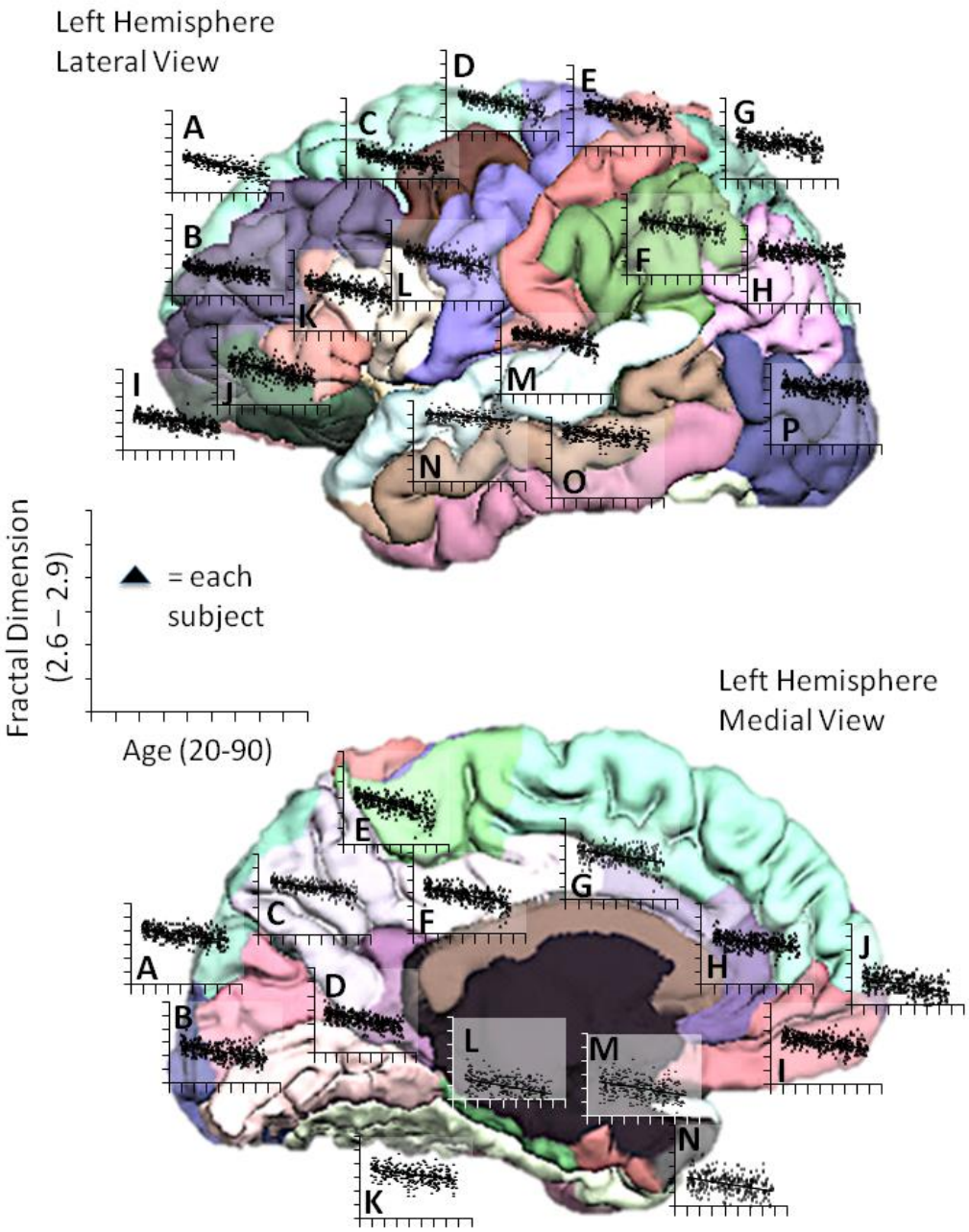

Figure 5.3 Change in fractal dimension across the lifespan for local regions of interest. ROI-specific values were computed by grouping cortical voxels that shared the same parcellation label, as determined by FreeSurfer. The mean fractal dimension (y-axis, using the same scale as in Figure 5.1) for each subject has been plotted with age along the x-axis (also the same scale as Figure 5.1) for each of the 34 regions of interest. The left hemisphere is displayed in this figure, with the left hemisphere lateral view in the upper panel (I) and left hemisphere medial view in the lower panel (II).

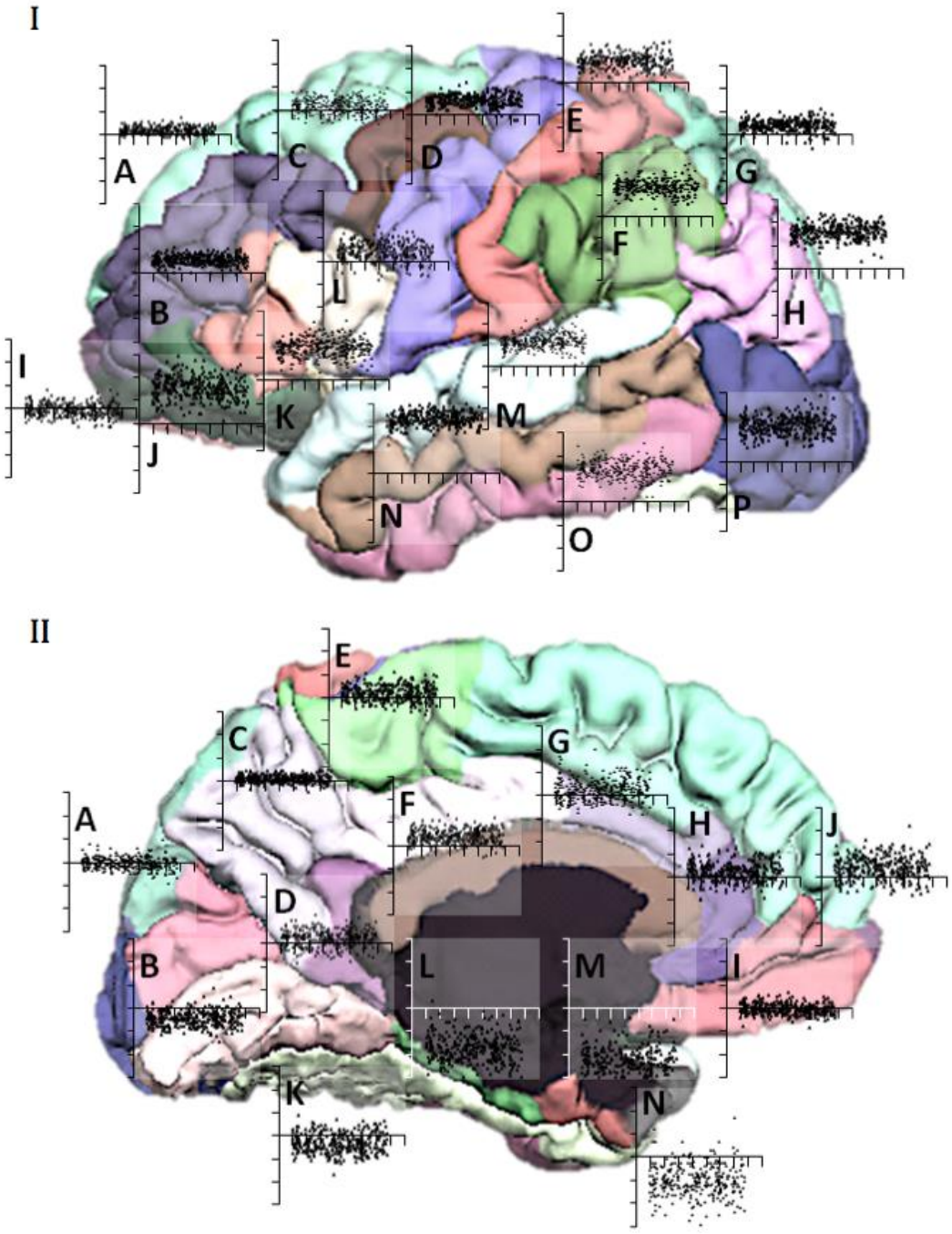

Figure 5.4 Asymmetry in fractal dimension across the lifespan for local regions of interest. The data are displayed using the same convention as Figure 5.3, except that the y-axis from each graph reflects the difference in ROI fractal dimension (left minus right, scale as shown in Figure 5.2). Considerable variability in ROI asymmetry is seen in this normal population.

Table 5.1 Average lobar values. The fractal dimension for each cortical voxel were aggregrated into lobes based upon the FreeSurfer cortical parcellation. Average values are shown for each lobe for the cohort in their 20s and in their 80s.

	Left Hemisphere			Right Hemisphere		
Lobe	Ave FD-20s	Ave FD-80s	Norm. %D	Ave FD-20s	Ave FD-80s	Norm. %D
Frontal	2.7365	2.6821	18.1*	2.7164	2.6647	17.2*
Parietal	2.7816	2.7355	15.4*	2.7401	2.6941	15.3*
Temporal	2.8135	2.7750	12.8*	2.7700	2.7342	12.0*
Occipital	2.7958	2.7600	11.9*	2.7630	2.7284	11.5*

*For all regions the t-test between the 20s cohort and the 80s cohort showed a p value <0.0001

Table 5.2 Average region-of-interest values. The fractal dimension for each cortical voxel were aggregrated into 35 cortical regions based upon the FreeSurfer cortical parcellation using the Desikan-Killiany atlas. Average values are shown for each region for the cohort in their 20s and in their 80s.

		Ave FD: Left Hemisphere			Ave FD: Right Hemisphere			Left - Right Norm. %D	
Lateral Surface Region label		20s	80s	Norm. %D	20s	80s	Norm. %D	20s	80s
A	Superior Frontal	2.729	2.662	22.7*	2.718	2.654	22.3*	3.5	2.7
B	Rostral Middle Frontal	2.711	2.675	13.2*	2.684	2.646	13.7*	9.0	9.6
C	Caudal Middle Frontal	2.701	2.654	17.0*	2.690	2.646	16.1*	3.6	2.8
D	Pre-Central	2.725	2.672	19.2*	2.697	2.642	20.1*	9.3	10.1
E	Post-Central	2.748	2.698	17.8*	2.702	2.651	18.8*	15.2	15.8
F	Supramarginal	2.802	2.761	14.7*	2.729	2.689	14.7*	24.4	23.8
G	Superior Parietal	2.752	2.709	15.5*	2.728	2.692	14.0*	8.0	5.7
H	Inferior Parietal	2.806	2.778	10.3*	2.728	2.697	12.3*	25.7	27.2
I	Lateral Orbitofrontal	2.728	2.687	14.3*	2.731	2.692	12.9*	-0.8	-1.8
J	Pars Orbitalis	2.759	2.703	17.9*	2.679	2.629	17.4*	26.6	24.6
K	Pars Triangularis	2.779	2.730	17.5*	2.708	2.661	17.6*	23.6	23.1
L	Pars Opercularis	2.778	2.727	18.1*	2.756	2.711	16.3*	7.3	5.4

Table 5.2 Continued

Lateral Surface Regional Label		Ave FD: Left Hemisphere			Ave FD: Right Hemisphere			Left - Right Norm. %D	
		20s	80s	Norm. %D	20s	80s	Norm. %D	20s	80s
M	Superior Temporal	2.824	2.776	16.8*	2.768	2.717	18.4*	18.7	19.6
N	Middle Temporal	2.852	2.829	8.1*	2.738	2.709	10.9*	38.0	39.9
O	Inferior Temporal	2.849	2.822	9.6*	2.777	2.747	10.3*	24.2	25.0
P	Lateral Occipital	2.822	2.796	9.7*	2.744	2.720	9.3*	26.2	25.5
Medial Surface Region label									
A	Cuneus	2.802	2.765	13.4*	2.803	2.771	11.2*	0.0	-1.8
B	Lingual	2.737	2.694	15.4*	2.758	2.715	15.4*	-7.0	-7.0
C	Precuneus	2.795	2.750	16.18	2.789	2.745	16.0*	2.1	1.6
D	Isthmus Cingulate	2.733	2.691	15.2*	2.721	2.677	16.3*	4.0	4.8
E	Para-Central	2.751	2.695	20.7*	2.740	2.681	20.8*	3.8	4.4
F	Posterior Cingulate	2.762	2.710	19.3*	2.743	2.690	19.1*	6.5	6.4
G	Caudal Anterior Cingulate	2.773	2.729	16.8*	2.762	2.714	17.7*	3.6	5.1
H	Rostral Anterior Cingulate	2.772	2.743	11.6*	2.765	2.728	12.2*	2.5	5.1
I	Medial Orbitofrontal	2.774	2.740	11.7*	2.776	2.743	11.0*	-0.6	-0.8
J	Frontal Pole	2.691	2.654	13.5*	2.682	2.637	14.6*	2.8	5.9
K	Fusiform	2.780	2.746	11.8*	2.794	2.757	12.4*	-4.6	-3.9
L	Parahippocampal	2.674	2.615	18.2*	2.750	2.711	12.0*	-25.3	-32.1
M	Entorhinal	2.715	2.668	15.5*	2.835	2.798	10.5*	-39.9	-43.5
N	Temporal Pole	2.696	2.656	13.4*	2.745	2.704	13.6*	16.5	16.0

*For all regions, the t-test between the 20s cohort and the 80s cohort showed a p value <0.005

CHAPTER 6

CONCLUSION

6.1 Summary of Contributions and Impact to Medical Imaging and Clinical Neurology

The overall objective of the independent research outlined in this dissertation has been to improve the process of interpreting neuroimages in the diagnosis of neurodegenerative diseases, particularly age-appropriateness, by quantifying and summarizing spatiotemporal patterns of age-related shape changes of the human cerebral cortex, which reflects the underlying anatomical changes due to normal aging. Several concepts and tools have been developed to meet this overall objective.

In Chapter 3, the use of global fractal dimension, i.e., one number that summarizes shape complexity for the entire cerebrum, is presented as an integrative marker to quantitatively characterize age-related changes in the shape of the cerebral cortex across the adult human lifespan. To account for the variability of cortical shape within age groups and improve the characterization of cortical shape change with normal aging, age-weighted

atlases were constructed in Chapter 4 for the age range of 20 to 89. The concept of vector energy within the Large Deformation Diffeomorphic Metric Mapping framework was used to quantify the variability within and the difference between age groups. A novel concept of fractal dimension-weighted atlases to better capture cortical shape change was also presented in Chapter 4. With the critical understanding of the focal nature of shape change in the cerebral cortex with normal aging and neurodegenerative diseases, tools were developed to quantify shape complexity on a voxel-by-voxel and regional scale (local fractal dimension). The use of local fractal dimension to quantitatively characterize lobar and regional age-related spatiotemporal changes in the shape of the cerebral cortex across the adult human lifespan was presented in Chapter 5.

Quantitative clinical tools built using the concepts and tools presented in this dissertation will have a significant impact on the practice of neurology, as subjectivity in the interpretation of structural imaging data would be replaced by an objective, quantitative metric in the characterization of age-appropriateness and diagnosis of neurodegenerative diseases for individuals. Secondly, using a quantitative imaging biomarker can detect pathological effects of AD during the presymptomatic period. Lastly, this tool has future applications to monitor the progression of disease and as a part of the selection/inclusion criteria, as a safety marker and as an outcome measure for clinical trials of disease-modifying targeted treatments.

Although these tools and methodologies have been initially applied to a cognitively normal population, these tools can be applied to any condition that causes a change in the shape of the cerebral cortex (i.e., traumatic brain injury or neurodegenerative diseases such as Alzheimer's disease and Lewy body dementia) or other fractal objects of interest.

6.2 Unpublished Results

The construction of atlases, as a statistical representation of a population, and using vector energy from the LDDMM framework to study similarity in shape using MR images have been extensively researched. Similarly, the relevance and use of fractal dimension has also been extensively researched. However, the application of unbiased diffeomorphic atlasing methodology to cortico-fractal surfaces to characterize complexity change in the shape of the cerebral cortex throughout the adult lifespan is a novel methodology.

This technique enables researchers to put the cortico-fractal surfaces into a common space enabling statistical inferences about intrapopulation variability, intrapopulation differences, spatiotemporal changes, and delineation analysis from neuropathology based upon cortical complexity. Fractal dimension as a metric summarizes and reflects clinically relevant anatomical state. The examination of fractal dimension changes reflects anatomical changes due to physiology and/or pathophysiology. Furthermore,

this technique can be translated for many applications, such as alignment of stereotactic surface projection (SSP) maps of brain positron emission tomography (PET) data.

The characterization of spatiotemporal patterns of local cerebral cortical complexity changes using diffeomorphic atlasing for cognitively normal individuals across the adult human lifespan would set a baseline for cortical shape changes with normal aging. The steps below outline the methodology that was used to complete this goal.

Age-weighted atlases were created for each half-decade and decade, as per Chapter 4. In addition to steps included in Chapter 4, the MR images of the individuals used for atlasing, FreeSurfer generated brainmasks, were masked with its original intensity values from the original MR. This is after each brainmask and original MR were conformed to the same size and reformatted to be type float. Then the brainmasks were intensity normalized with respect to the cohort used. This is as opposed to using brainmasks, which have been intensity normalized by FreeSurfer, and then intensity normalizing those images with respect to the cohort for atlasing. Masking the brainmasks to the original intensity values maintains the differentiation in intensity values for each tissue class in the brain, i.e., white matter, gray matter, and cerebrospinal fluid.

Each cortico-fractal surface is reformatted, resized, and reoriented. Transformations from each individual brain to the affine aligned space and

deformations from each individual brain to its respective MR atlas (atlas space) were computed using AtlasWerks. These transformations and deformations were applied to the cortico-fractal surfaces for each individual, which were generated using C^3. Voxel-by-voxel mean and standard deviation cortico-fractal surfaces were created using the individual deformed cortico-fractal surfaces (see Figure 6.1). Each half-decade and decade atlas was deformed to the successive. This deformation was computed and applied to the respective cortico-fractal surfaces. Thereafter, voxel-wise statistical significance maps between decades were created by calculating Z-scores (Z = [normal mean value] – [individual value]/normal SD) between the voxel-by-voxel mean cortico-fractal surfaces per decade. The Z-score calculation shows how many standard deviations the datum at each voxel is from the mean value at that particular voxel.

The statistical significance maps characterize spatiotemporal changes of local cerebral cortical fractal dimension with normal aging across the adult human lifespan.

6.3 Future Work

6.3.1 Validation and Comparison of Normal Aging Characterization Data

An atlas from DLBS subjects will be compared to age-matched Alzheimer's Disease Neuroimaging Initiative (ADNI) control subjects using a voxel-by-voxel correlation coefficient called eta^2 [1]. This provides an

important validation of the atlas-building technique and demonstrates the equivalence of the two databases.

For the ADNI database, multiple regression will performed to identify which factors are most strongly associated with changes in fractal dimension. These factors include demographics (e.g., age, gender, education, ethnicity), neuropsychologic testing results (e.g., MMSE, CDR-sum of boxes, ADAS-cog, CVLT-delayed recall, phonemic fluency), and MRI volumetric measures (e.g., hippocampal volume, whole brain volume, inferior lateral ventricular volume, cortical thickness, gyrification index).

6.3.2 Evaluation of Age-Calibrated Fractal Dimension as a Neuroimaging Biomarker for AD

Statistical analysis will proceed using the same procedure as Section 6.3.1, with the addition of blood/CSF biomarkers (e.g., APOE-e4 status, CSF Amyloid $b_{1\text{-}42}$ levels, CSF Tau levels) from the ADNI database.

Voxel-by-voxel Z-score maps will be produced based upon comparing individuals to age-matched ADNI control subjects. Multivariate analysis of fractal dimension Z-score maps will be produced using partial least squares regression (PLS). PLS assumes that there is noise in the predictor variables (FD Z-score). The outcome variable will be diagnosis as normal, MCI, or AD. The latent variable that will be produced by the PLS analysis is the

topographical distribution of complexity changes. PLS is particularly well suited when the predictor variable is high dimensional and the outcome variable (diagnosis) is low dimensional. After a PLS model is built on training data (from a subset of ADNI), a new subject's FD Z-score map can be input to produce a score of cortical complexity, where a low score will represent an complexity pattern similar to control subjects and a higher score a pattern indicative of Alzheimer's disease. Effect sizes for the fractal analysis will also be compared to standard volumetric measures.

6.3.3 Dissociation of Shape Changes with Normal Aging from AD

Statistical significance maps will be created for a cohort of Alzheimer's disease individuals from the ADNI database by following the methodology described in Section 6.2 of this chapter. This results in the signature spatiotemporal changes in cerebral cortical shape complexity associated with Alzheimer's disease.

Age-matched atlases of normal individuals and individuals with Alzheimer's disease will be deformed to the same space. These deformations will be applied to the cortico-fractal surfaces and statistical significance maps will be generated to dissociate spatiotemporal changes in cerebral cortical shape complexity associated with normal aging from those caused by Alzheimer's disease. An example is shown in Figure 6.2.

This methodology will be applied to every disorder in the dementia spectrum to characterize signature spatiotemporal changes in cerebral cortical shape complexity associated with each disease to distinguish between each disease.

6.3.4 Classification of Cognitively Normal Individuals and Individuals with AD Using Local FD

The application of unbiased diffeomorphic atlasing methodology to cortico-fractal surfaces to characterize local spatiotemporal changes in cerebral cortical shape complexity may increase the sensitivity and specificity of the classification of an individual as cognitively normal versus diseased. The statistical significance maps generated to dissociate spatiotemporal changes in cerebral cortical shape complexity associated with normal aging from those caused by Alzheimer's disease will be used to train on half an independent test population to create a cut-off between cognitively normal and AD.

Following training, the spatiotemporal patterns of cortical complexity loss will be used to differentiate between cognitively normal individuals and individuals with AD on the other half of the dataset using the cut-off generated with the training set. The accuracy of differentiation will be determined by area-under-the-curve analysis.

6.3.5 Evaluation of the Effects of Common Co-Morbidities on Age-Calibrated FD

Ongoing studies in the University of Utah Geriatrics Clinic and Cognitive Disorders Clinic have developed sophisticated mechanisms to enroll subjects into imaging studies. This proposal will take advantage of the established infrastructure to prospectively enroll subjects with cognitive complaints. Subjects enrolling in this observational study will have completed a detailed cognitive evaluation including medical history, neurological examination, routine screening laboratory tests, and a neuropsychological test battery. Based upon previous clinical experience, approximately half of the subjects seeking evaluation will not have undergone evaluation with MR imaging. These subjects will get a MRI (including the necessary MP-RAGE sequence) at the University of Utah as a routine part of their clinical evaluation. The other half will have been imaged at an outside facility. While the MR images are generally sufficient for the clinical evaluation, they typically do not include a high-quality MP-RAGE sequence. These subjects will need to obtain the MP-RAGE (and FLAIR) image sequence for research purposes. An additional collection of demographic data (using the ADNI template) will be collected at the time of enrollment. All procedures and protocols will be approved by the University of Utah IRB prior to subject recruitment and enrollment. Inclusion and exclusion criteria will be based upon ADNI, with the requirements for

medication use and co-morbid conditions waived. Subjects will be segregated into clinical categories (AD, MCI, or control) based upon the clinical diagnosis given in the Cognitive Disorders Clinic. The recruitment goal will be 30 subjects per clinical category (90 subjects total) over 2 years.

Multivariate regression will process in the same manner as described in Section 6.3.1, with the addition of new demographic (e.g., medications, Hachinski ischemic index, functional activity questionnaire), medical (e.g., thyroid function tests, creatinine, Geriatric Depression Scale) and imaging (e.g., white matter hyperintensity volume) parameters. Factors having large regression coefficients with cortical FD will be identified for additional study in future prospective trials.

6.3.6 Integration of Structural, Metabolic, and Pathological Information

While all three imaging biomarkers, Amyloid-PET, FDG-PET, and fractal MR, have shown promise in identifying patients with neurodegenerative disease, each has advantages and disadvantages to their use. Combining the complementary information contained in each of these biomarkers could greatly increase the diagnostic confidence in the result. For example, Amyloid-PET is very sensitive at detecting the presence of Amyloid plaques associated with AD. As many cognitively healthy elderly subjects show evidence of significant plaque burden, the presence of amyloid alone is

of undetermined significance [2]. However, evidence of amyloid together with structural neurodegeneration and cortical hypometabolism could be a strong indicator of impending disease. This highlights the value of an integrated measure.

Our lab has been successful in creating cortical maps for Amyloid-PET, FDG-PET, and fractal MR, each of which has been analyzed to compute a Z score for each voxel. These voxels will be then aligned using the diffeomorphic atlasing tool. There are many ways to create a composite index. The initial method that will be used has been used in other studies of compositing neuroimaging data [3]. The composite Z-score (CoMPS) for each voxel equal to the summed Z-scores divided by the pooled standard deviation of the composited tests (Equation 6.1),

$$CoMPS = \frac{Z_M + Z_P + Z_S}{\sqrt{\sigma_M^2 + \sigma_P^2 + \sigma_S^2 + 2(r_{MP} + r_{MS} + r_{PS})}} \tag{6.1}$$

where M,P, and S indicate the metabolic (FDG-PET), pathologic (Amyloid-PET), and structural (Fractal MR) analyses, respectively, s^2 is the variance, and r_{xy} is the correlation between tests x and y. The CoMPS index can be analyzed on a global-, regional-, or single voxel-level.

The research presented in the preceding chapters, the unpublished work section, and the future work section has been conceptualized, designed, and executed in an effort to continue to improve the standard of care provided to the patients suffering with neurodegenerative diseases.

6.4 References

[1] A. Cohen, D. Fair, N. Dosenbach, F. Miezin, D. Dierker, D. Van Essen, B. Schlaggar and S. Petersen, "Defining functional areas in individual human brains using resting functional connectivity MRI," NeuroImage, vol. 41, no. 1, pp. 45-57, 2008.

[2] W. Jagust, "Amyloid imaging: Coming to a PET scanner near you," Annals of Neurology, vol. 68, no. 3, pp. 277-278, 2010.

[3] A. Poonawalla, S. Datta, V. Juneja, F. Nelson, J. Wolinsky, G. Cutter and P. Narayana, "Composite MRI scores improve correlation with EDSS in multiple sclerosis," Multiple Sclerosis, vol. 16, no. 9, pp. 1117-1125, 2010.

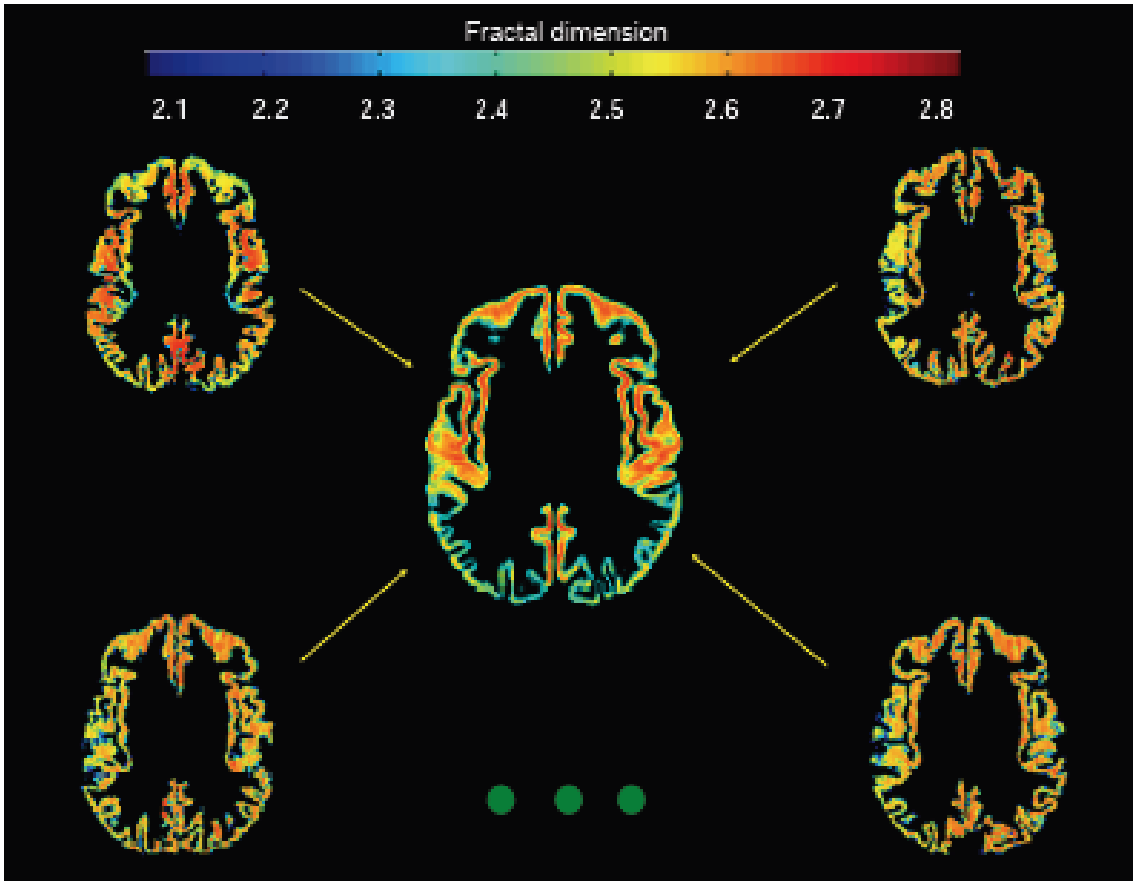

Figure 6.1 Construction of voxel-based cortico-fractal surface mean. Application of individual MRI-based deformation fields to deform the respective cortico-fractal surfaces to the atlas space. Voxel-by-voxel mean and standard deviation cortico-fractal surfaces were created using the individual deformed cortico-fractal surfaces.

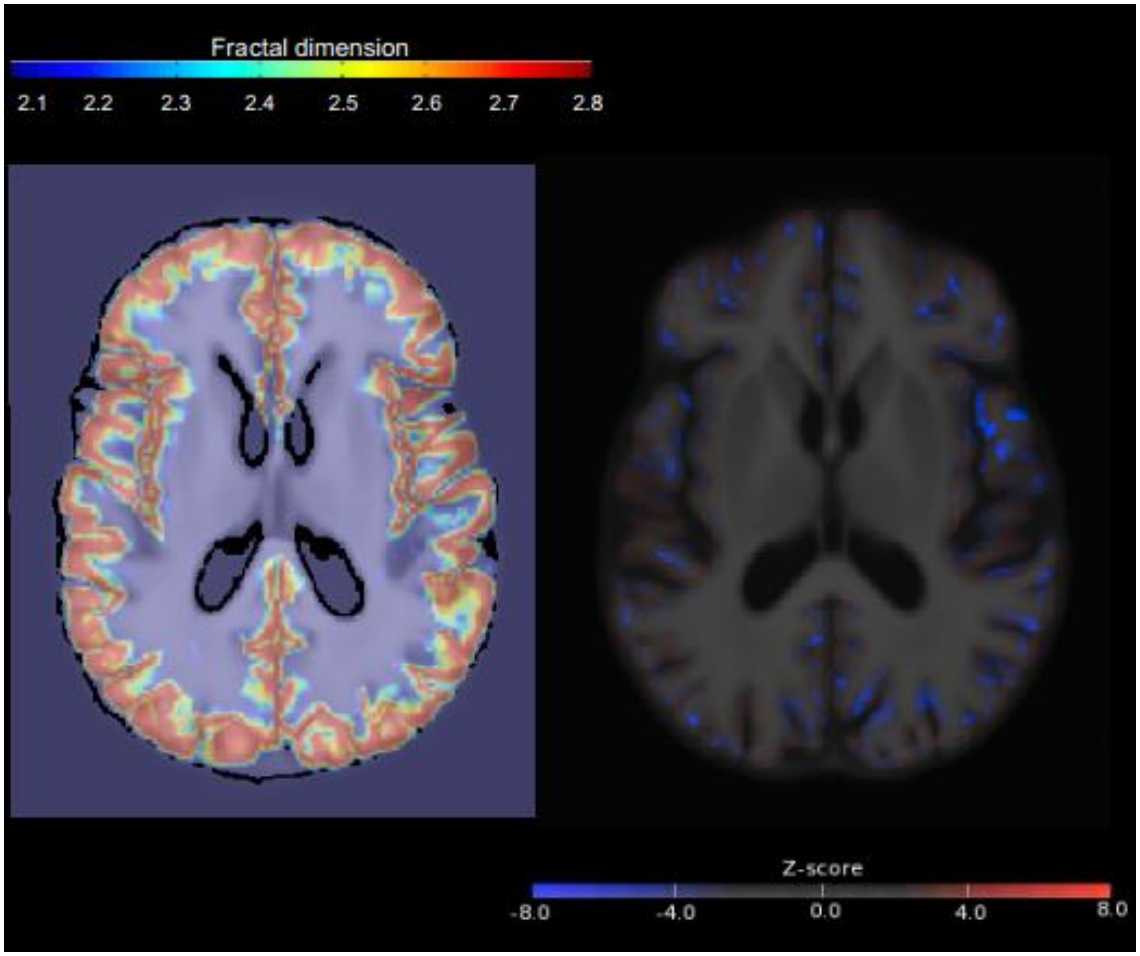

Figure 6.2 Example of application of Z-score for AD. Fractal surface of 1 AD subject aligned and superimposed onto the Atlas of the 68 cognitively normal subjects (left panel). Statistics were computed on a voxel-by-voxel basis to generate Z-score maps. In this case, the Z-score represents the difference in shape complexity at each voxel of the individual AD subject with respect to the mean value of complexity of the cognitively normal atlas at that particular voxel (right panel).